

Geophysical Fluid Dynamics: from the Lab, up and down!

Henri-Claude Nataf

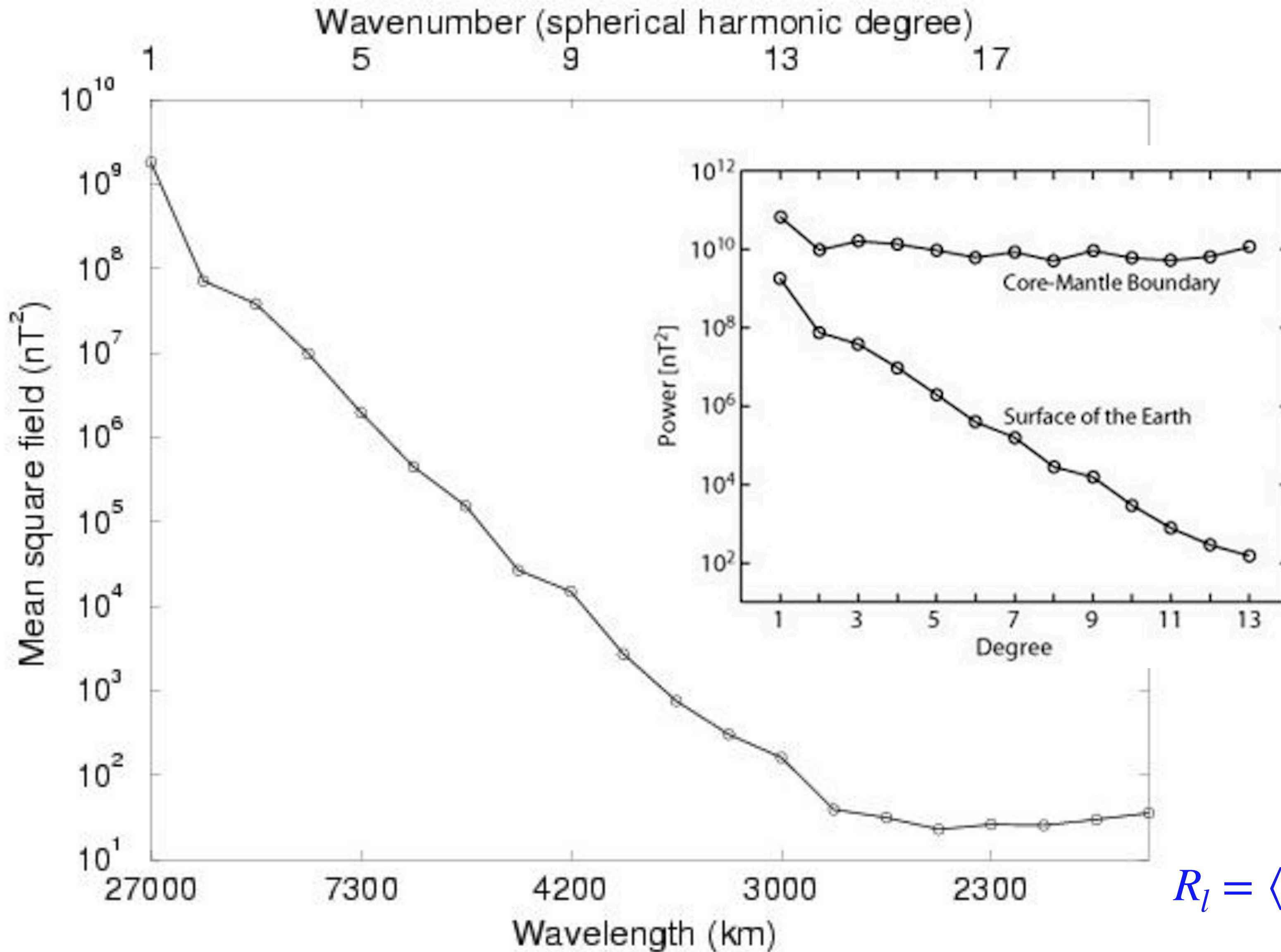
Univ Grenoble Alpes / CNRS
Grenoble, France

Fluid Dynamics in Earth and Planetary Sciences

Kyoto, November 27-30, 2018



The spectrum of the Earth's magnetic field



- This shows the Lowes **power spectrum** of the Earth magnetic main field as a function of degree l . Beyond $l = 13$, the spectrum of the field at the surface levels off, due to **crustal contributions**.

- At the CMB, the low degree spectrum is **flat**; the **dipole** stands out.

$$R_l = \langle B_l^2 \rangle = (l + 1) \sum_{m=0}^l \left(\frac{a}{r} \right)^{2l+4} [(g_l^m)^2 + (h_l^m)^2]$$

3.4. Core flows

Frozen-flux

- The **secular variation** of the magnetic field observed at the CMB is related to the **flow at the surface of the core** (just beneath the Ekman layer). Indeed, considering the radial component of the magnetic induction, we get:

$$\frac{\partial B_r}{\partial t} = - \nabla_H \cdot (\mathbf{u}_H B_r) + \frac{\eta}{r} \nabla^2 (r B_r)$$

where \mathbf{u}_H is the horizontal flow, and ∇_H the horizontal nabla operator.

- At short time scales (say decades or centuries), magnetic diffusion is weak, and one can use the **frozen-flux** approximation, leading to:

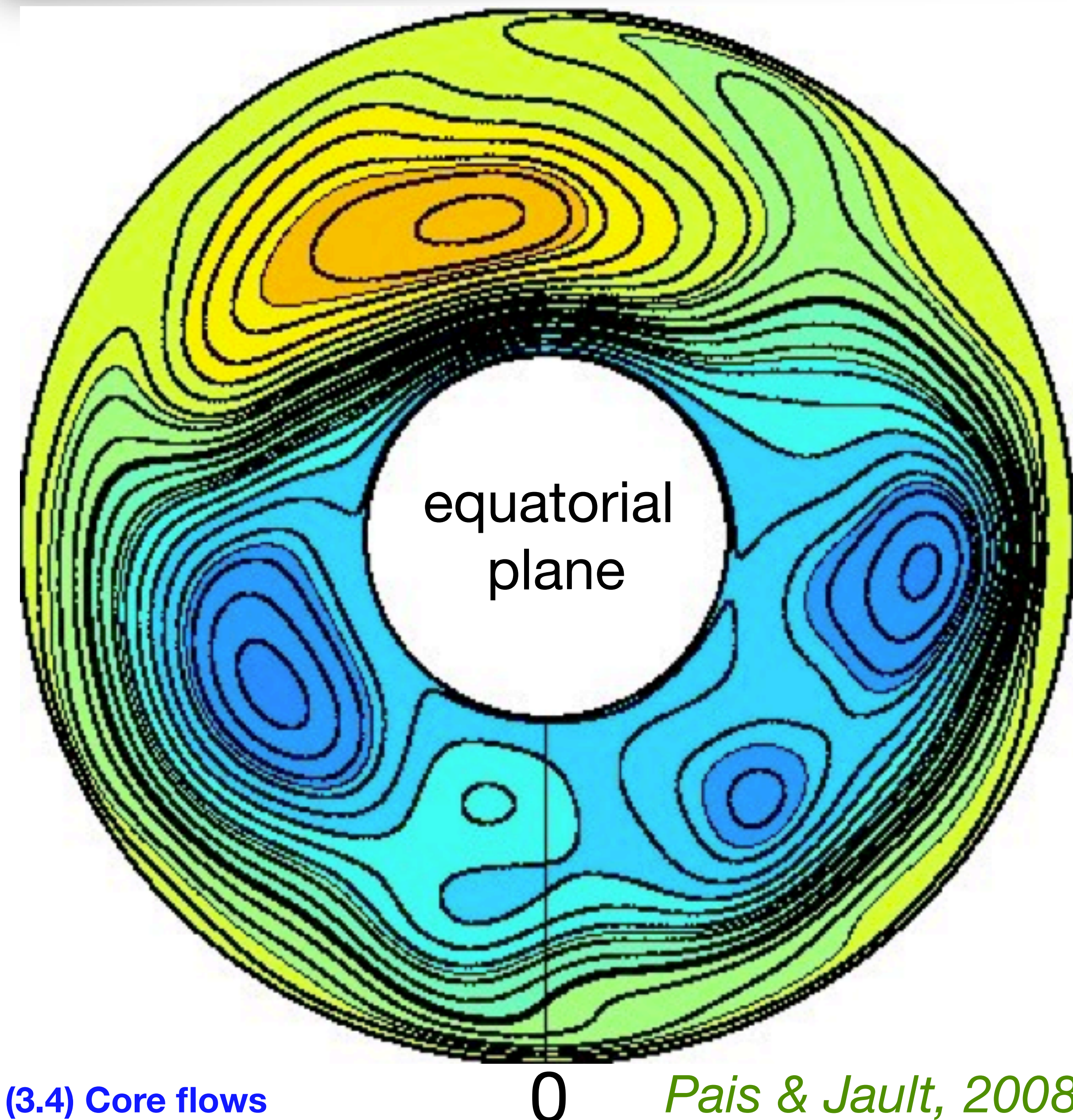
$$\frac{\partial B_r}{\partial t} = - \nabla_H \cdot (\mathbf{u}_H B_r)$$

see Holme, 2015

Constraints from the dynamics of rotating fluids

- Knowing the magnetic field at the CMB and its time derivative, one can access the **horizontal flow** at the surface of the core. However, the inversion is not unique, and only provides the surface flow.
- In the past decade, two elements have enabled a great progress:
 - 1) what we know of the dynamics of rotating fluids suggests that flow in the core would be **quasi-geostrophic**. This proves to be a very important and efficient constraint (Pais & Jault, 2008).
 - 2) **stochastic methods** using spectral and correlation information from observations and simulations yield an estimate of hidden contributions, providing more robust core flow inversions (Gillet et al, 2010).

A giant off-centered anti-cyclone



- Inversions of the secular variation (here for year 2000) with these constraints reveal a **giant off-centered anti-cyclone** in the Atlantic hemisphere.
- The stream function of the flow in the equatorial plane is shown here. Blue colors are for anti-cyclonic flow. The mean velocity is about **15 km/year**. (it takes about 300 years for one eddy turn-over time).

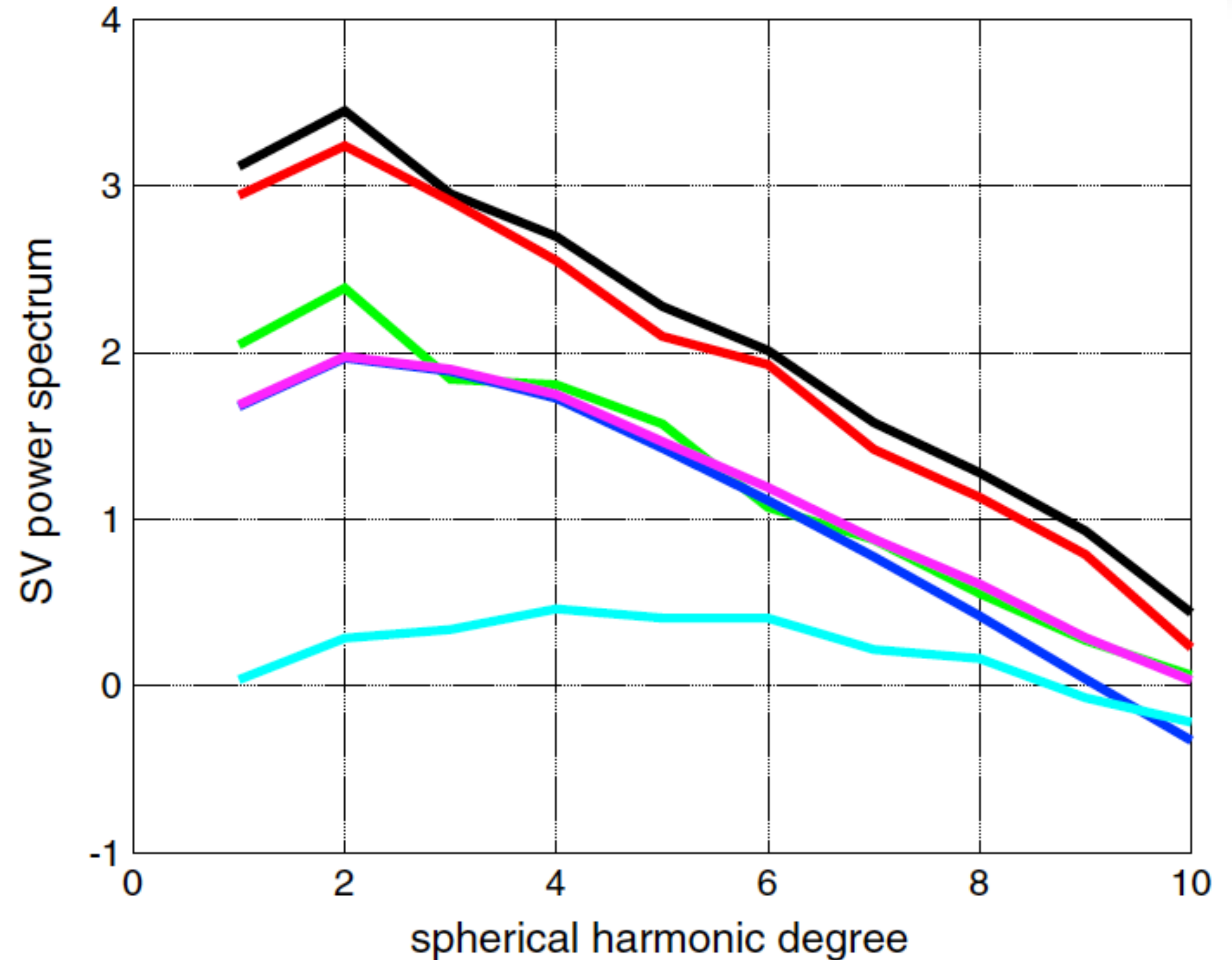
The effect of unresolved scales

$$\frac{\partial B_r}{\partial t} = - \nabla_H \cdot (\mathbf{u}_H B_r)$$

- Like what we have seen for the dynamo problem with Cowling's theorem and the mean field theory, we have to be careful about the inversion of core flow from the secular variation.
- Indeed **unresolved small scales** of \mathbf{u}_H and B_r can contribute to the **large scale** $\mathbf{u}_H B_r$ term. Therefore, we should not try to fit the observed secular variation within the observational error bars alone.

The magnetic secular variation spectrum

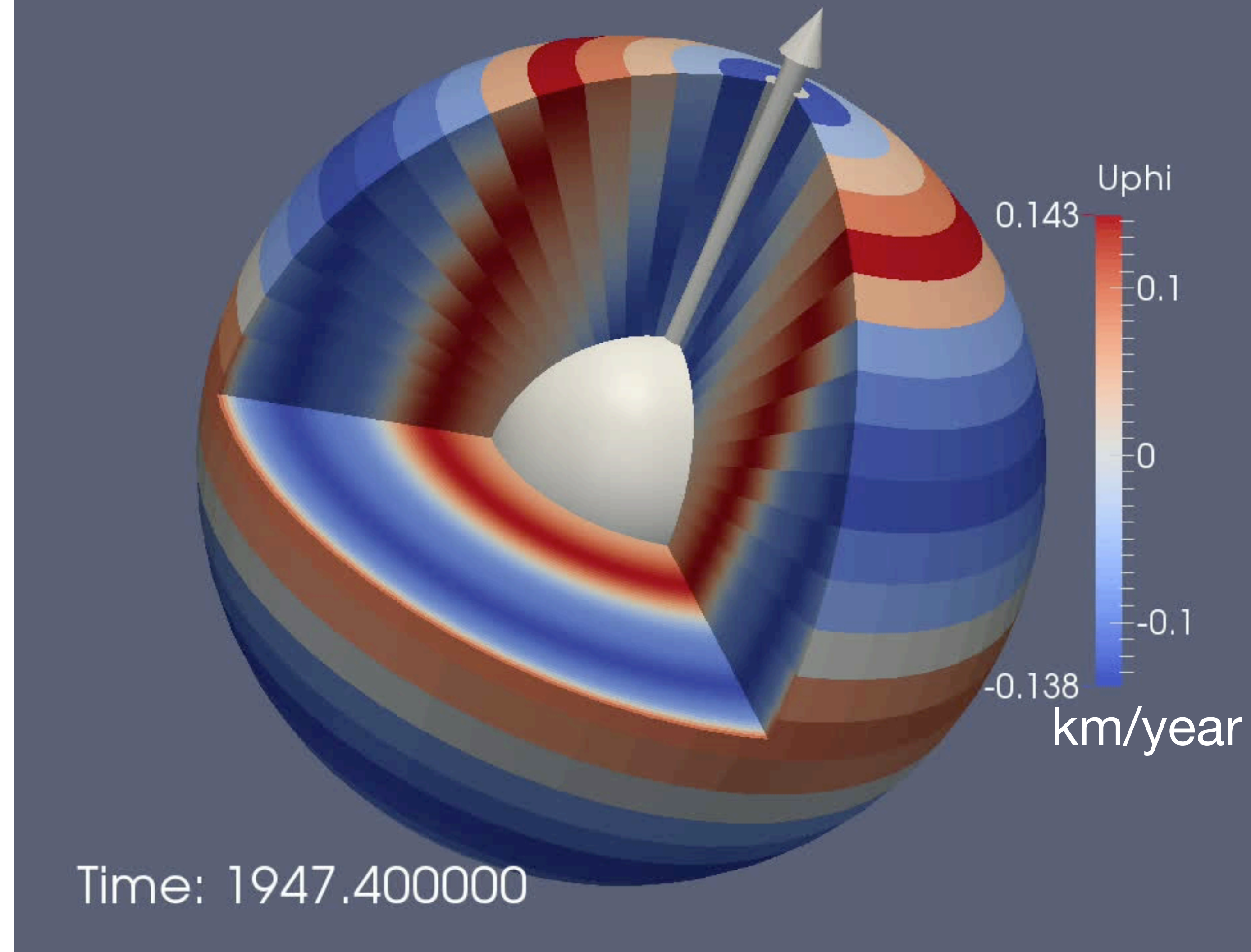
- SV power spectra at the Earth's surface, time averaged over 1940–2010 (scale is \log_{10} , in units of $(\text{nT}/\text{yr})^2$):
 - ▶ **black**: SV spectrum from COV-OBS.
 - ▶ **cyan**: associated observation errors.
 - ▶ **red**: ensemble average of the SV spectra for the model predictions.
 - ▶ **green**: model prediction errors.
 - ▶ **dark blue**: SV model errors due to unresolved scales.
 - ▶ **magenta**: the SV model errors plus observation errors.



Geostrophic Alfvén waves

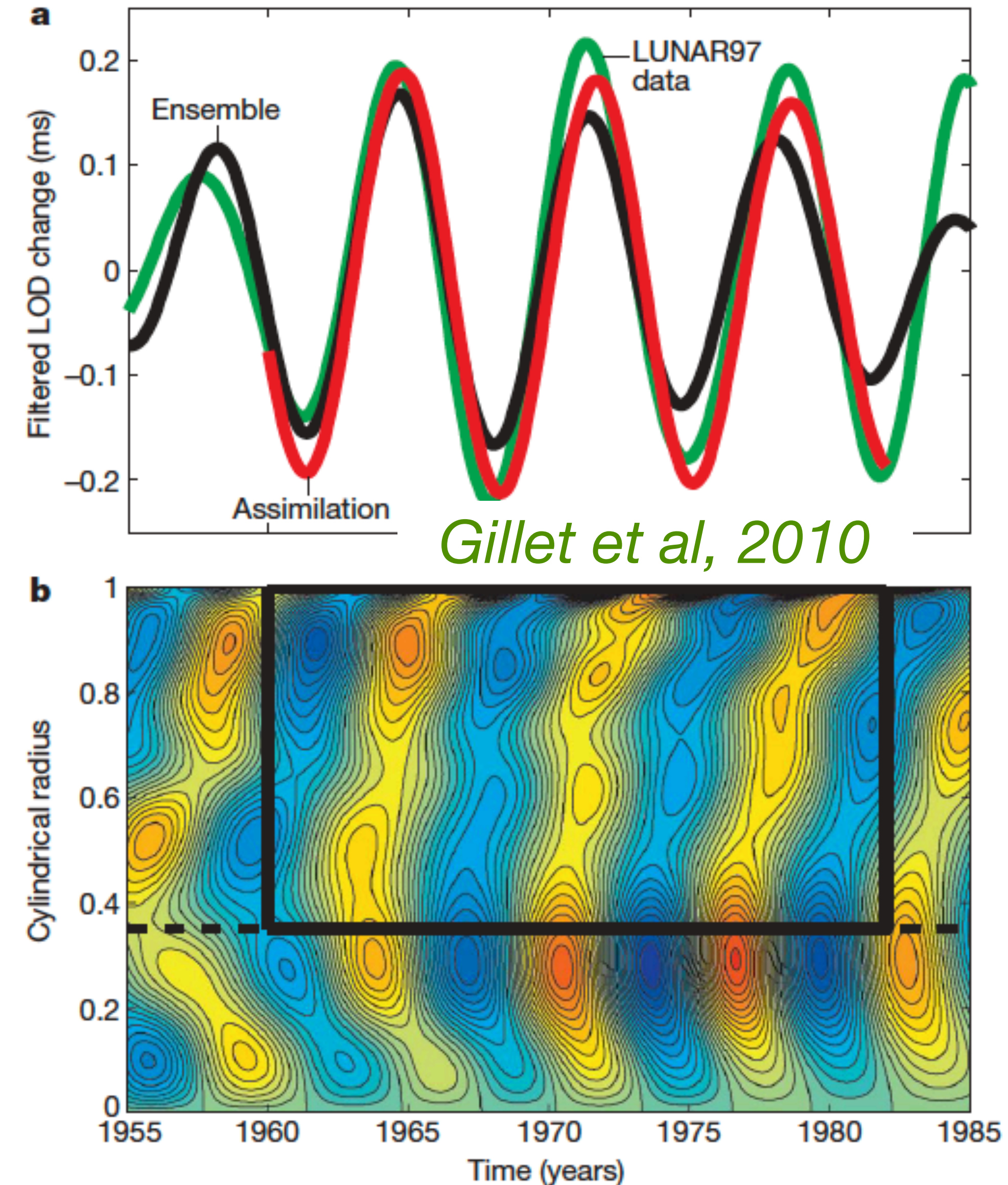
- This approach also led to the discovery of **geostrophic Alfvén waves** in the Earth's core (Gillet et al, 2010).
- I will present **Alfvén waves** and **geostrophic Alfvén waves** during my research seminar on Friday.
- In the core, it takes about **4 years** for these waves to cross the liquid core.
- This implies a magnetic field intensity of about **3 mT** inside the core.

from Gillet et al, 2010



Explaining the length-of-day variations

- These geostrophic Alfvén waves **exchange angular momentum with the mantle**, yielding variations of the **length-of-day (LOD)**.
- The excellent agreement found between the observed LOD signal and the signal predicted independently from the core flow is a strong confirmation of the **validity of the quasigeostrophic approach**.
- Comparing the time-constants of flow (300 years) and magnetic field (3 years), we conclude that the **magnetic energy** in the core is some **10 000 times** larger than the **kinetic energy**.



3.4.2. Alfvén waves

Alfvén waves

- A few words on Alfvén waves. Discovered by Hannes Alfvén in 1942, they are hydromagnetic waves, coupling the Navier-Stokes and the magnetic induction equation. They propagate along magnetic field lines.
- Let's assume an imposed uniform magnetic field \mathbf{B} and a fluid at rest, and let's have small velocity \mathbf{u} and magnetic \mathbf{b} perturbations.
- The linearized Navier-Stokes and induction equations become:



$$\rho \frac{\partial \mathbf{u}}{\partial t} = -\nabla p + \left(\frac{\mathbf{B}}{\mu} \cdot \nabla \right) \mathbf{b} + \rho \nu \nabla^2 \mathbf{u},$$
$$\frac{\partial \mathbf{b}}{\partial t} = (\mathbf{B} \cdot \nabla) \mathbf{u} + \frac{1}{\mu \sigma} \nabla^2 \mathbf{b}$$

Alfvén waves

- Introducing the Elsasser variables: $\mathbf{u}^{\pm} = \mathbf{u} \pm \mathbf{b}/\sqrt{\rho\mu}$

$$\frac{\partial \mathbf{u}^+}{\partial t} = -\nabla \frac{p}{\rho} + \left(\frac{\mathbf{B}}{\sqrt{\rho\mu}} \cdot \nabla \right) \mathbf{u}^+ + \nu \nabla^2 \mathbf{u} + \frac{1}{\mu\sigma} \nabla^2 \frac{\mathbf{b}}{\sqrt{\rho\mu}},$$

$$\frac{\partial \mathbf{u}^-}{\partial t} = -\nabla \frac{p}{\rho} - \left(\frac{\mathbf{B}}{\sqrt{\rho\mu}} \cdot \nabla \right) \mathbf{u}^- + \nu \nabla^2 \mathbf{u} - \frac{1}{\mu\sigma} \nabla^2 \frac{\mathbf{b}}{\sqrt{\rho\mu}}$$

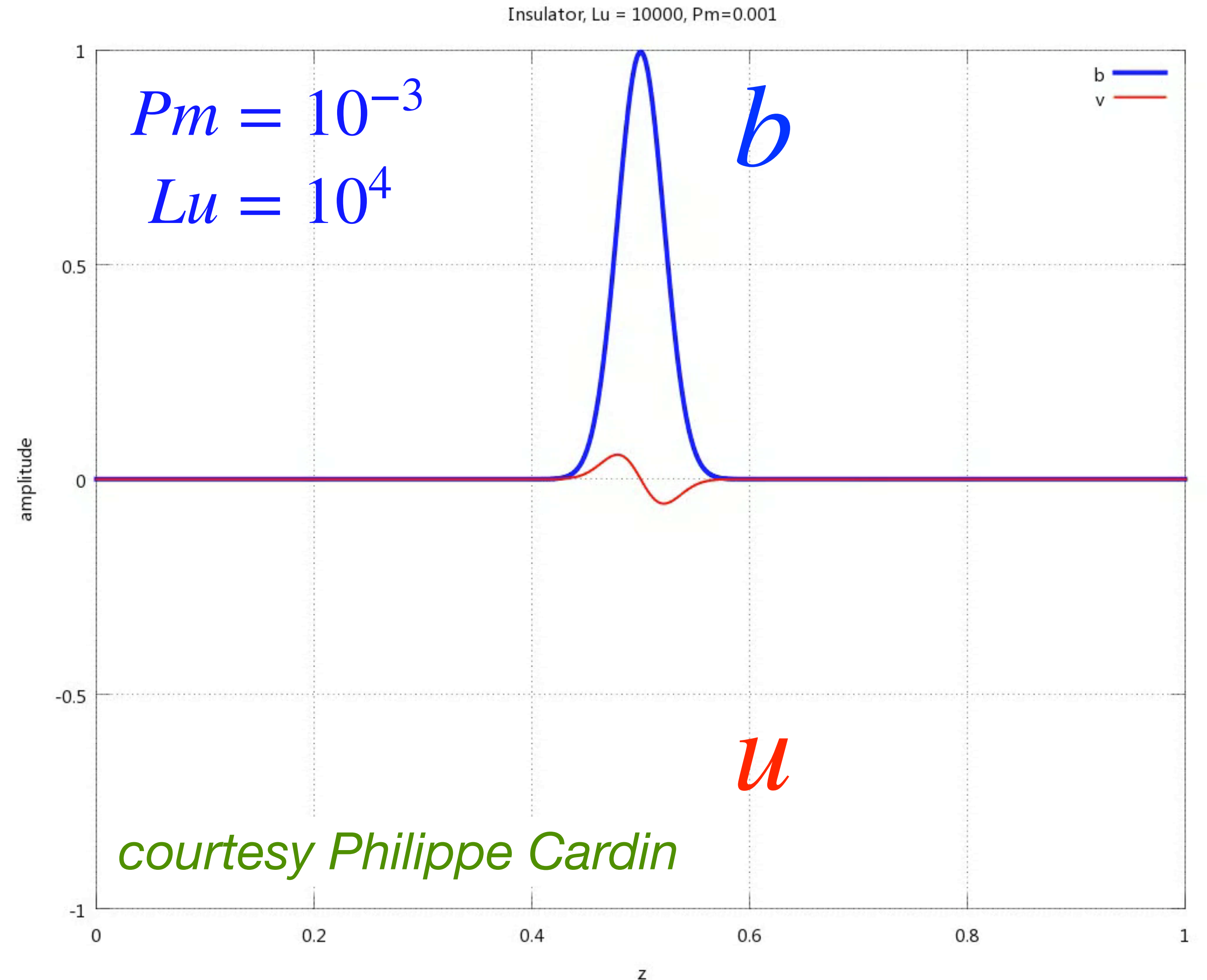
- In the absence of dissipation ($\nu=0$, $\eta=0$), we obtain a wave equation:

$$\frac{\partial \mathbf{u}^{\pm}}{\partial t} = \pm \left(\frac{\mathbf{B}}{\sqrt{\rho\mu}} \cdot \nabla \right) \mathbf{u}^{\pm}$$

Alfvén waves

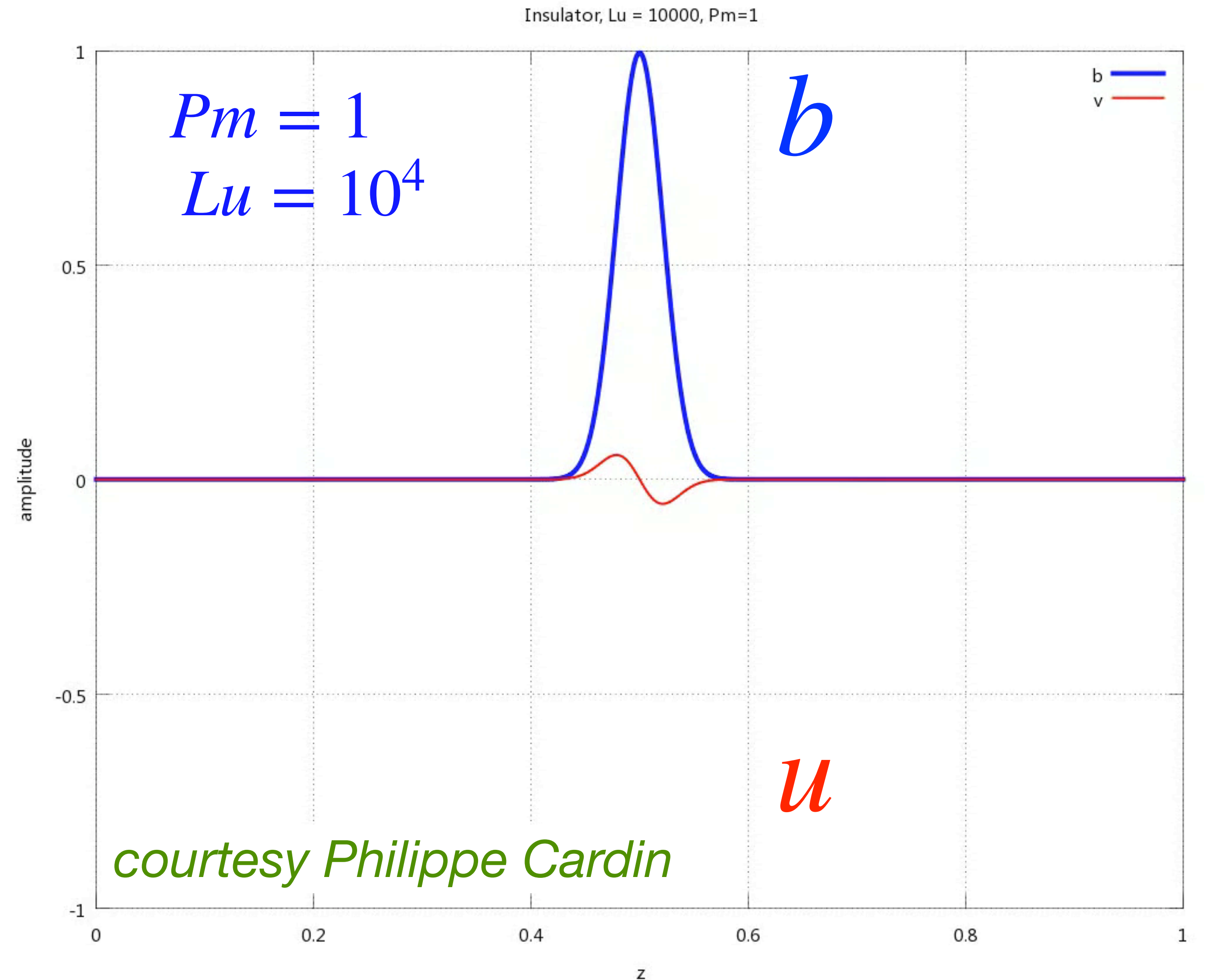
- Ideal (ie, non-dissipative)
Alfvén waves are:
 - ✓ transverse
 - ✓ non dispersive
 - ✓ equi-partitioned
 - ✓ travel at the **Alfvén velocity**

$$V_A = \frac{B}{\sqrt{\rho\mu}}$$



amazing Alfvén waves!

- An amazing phenomenon is observed when an Alfvén wave hits an **insulator boundary**, when the **magnetic Prandtl number is unity**.

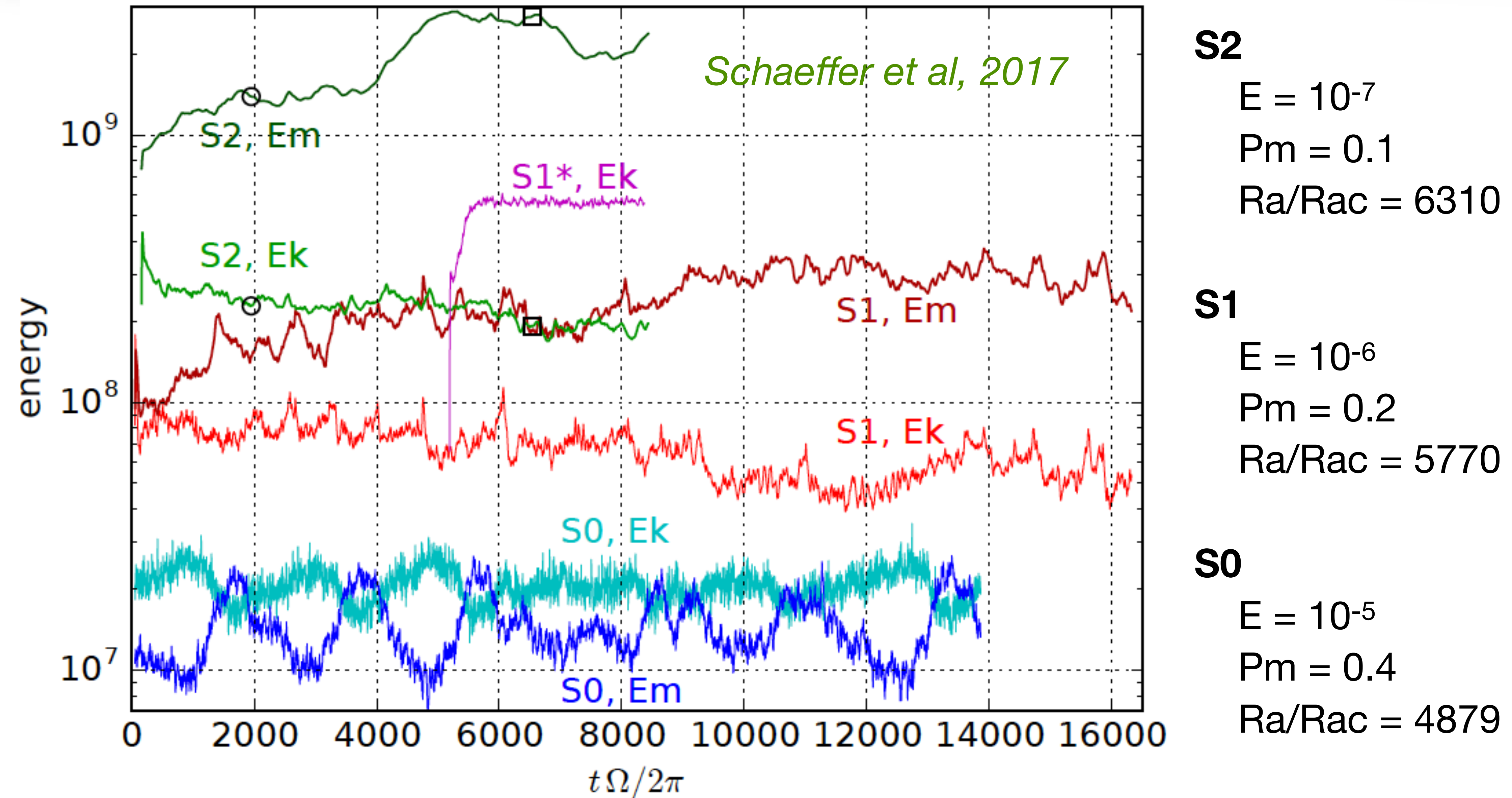


3.5. Numerical simulations of the geodynamo

Numerical simulations of the geodynamo

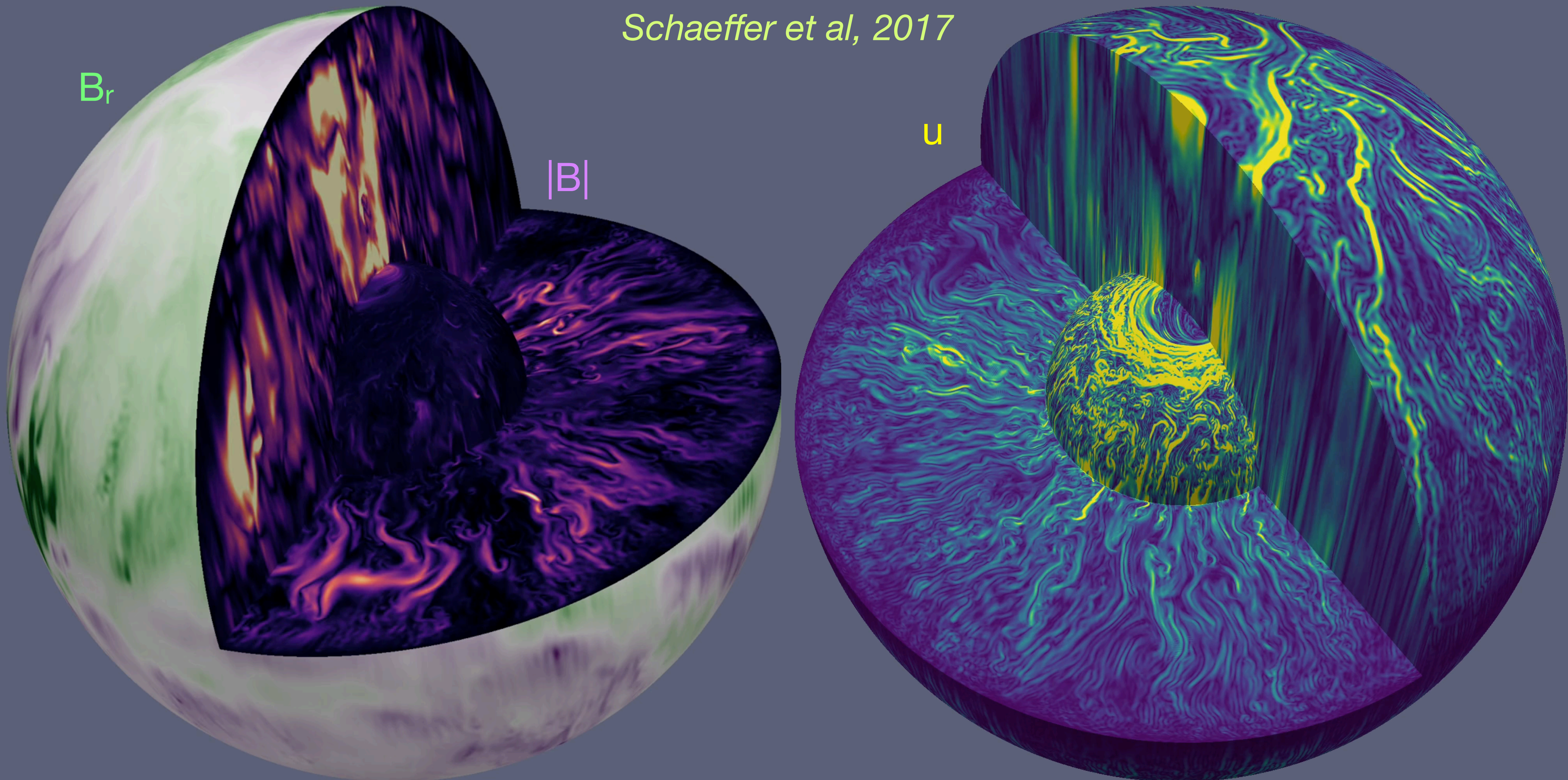
- I will not review the large literature of **numerical simulations of the geodynamo**, which started with the **landmark study of Glatzmaier and Roberts, 1995**.
- I would only like to share with you the lessons and beauty of one of the most extreme simulation recently published by Schaeffer *et al*, 2017. One goal of this simulation was to enter the regime in which the **magnetic energy is much larger than the kinetic energy**.

A large E_M/E_K dynamo simulation



Nathanaël Schaeffer's S2 dynamo

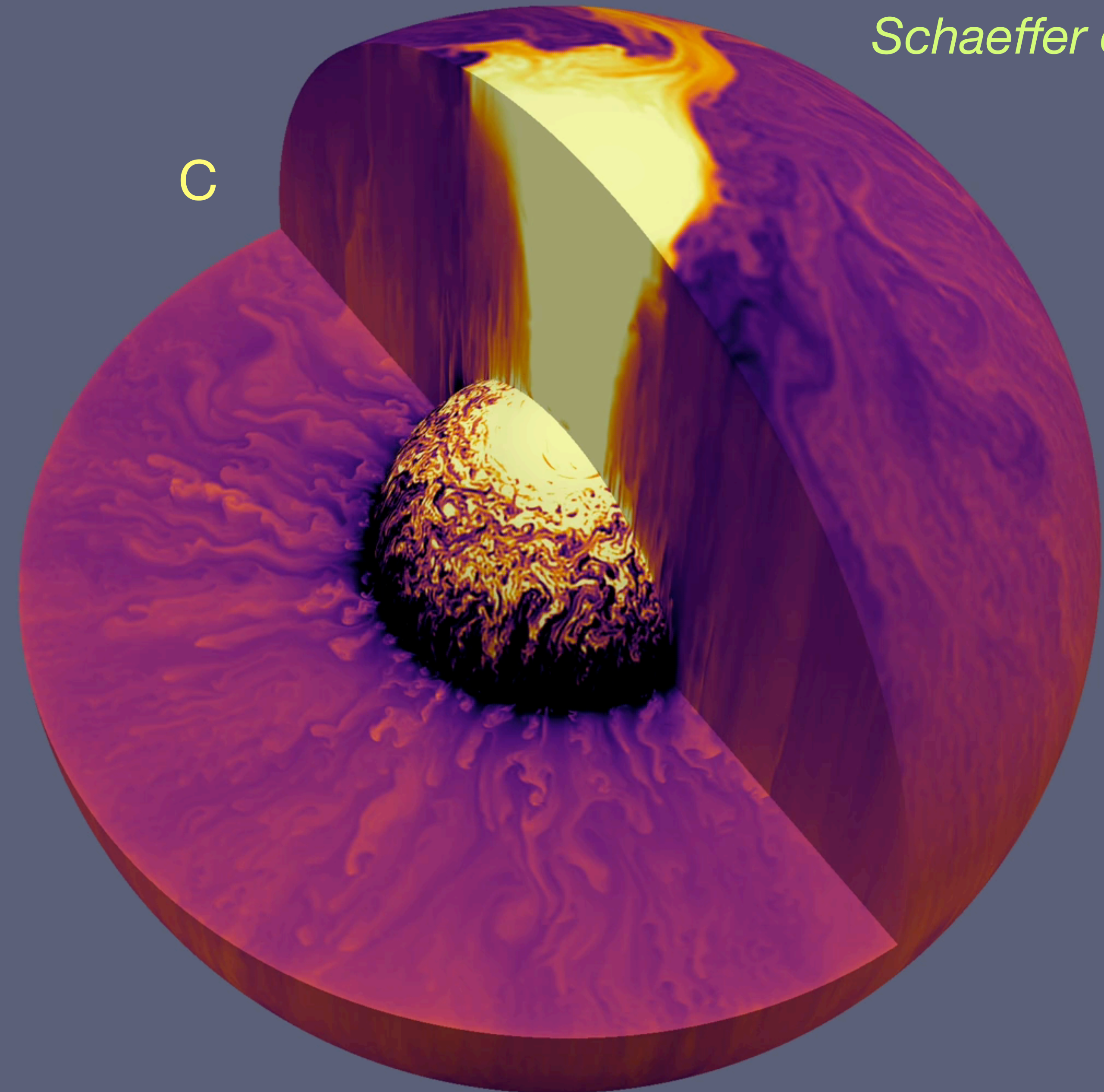
Schaeffer et al, 2017



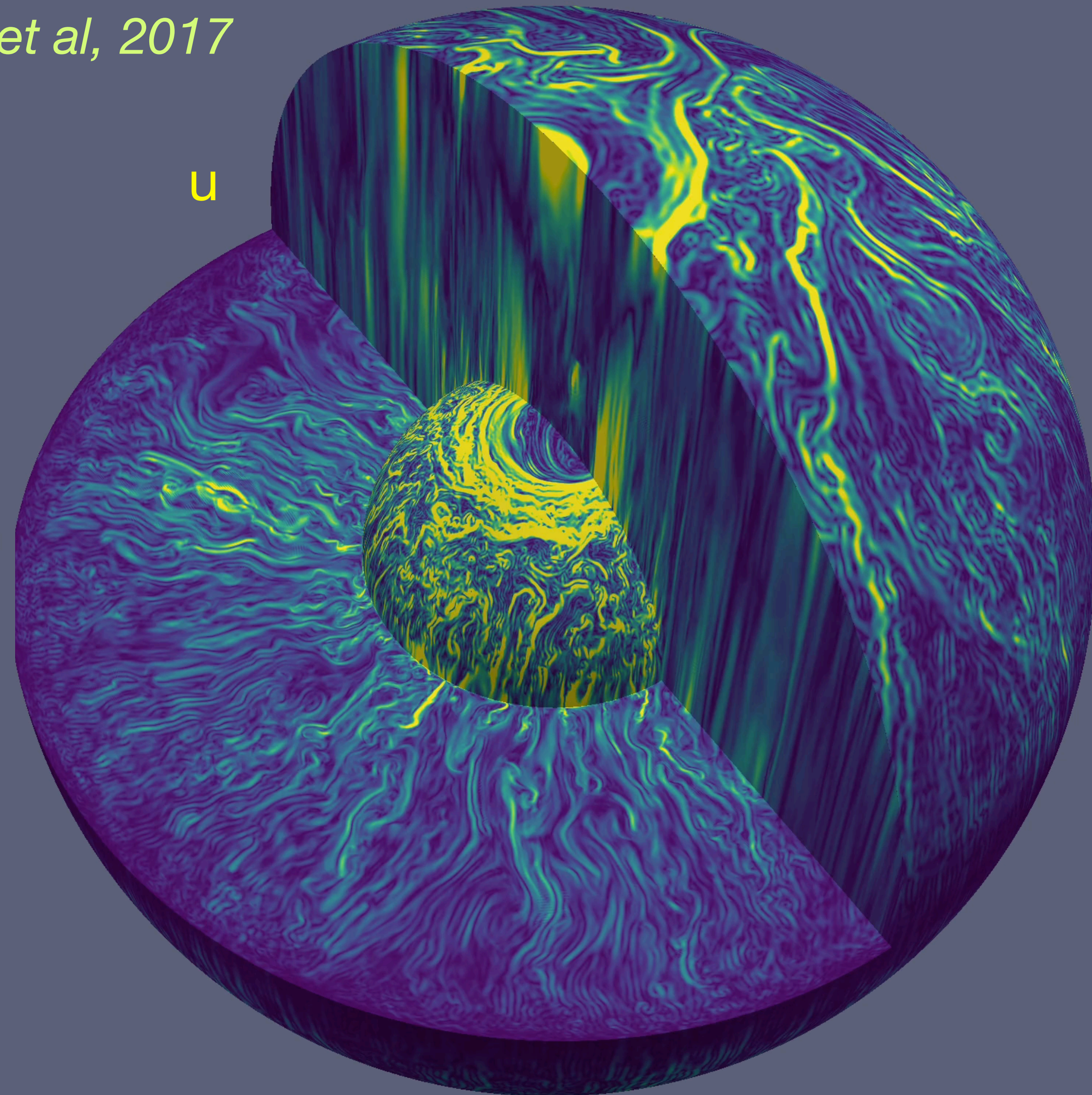
Nathanaël Schaeffer's S2 dynamo

Schaeffer et al, 2017

C

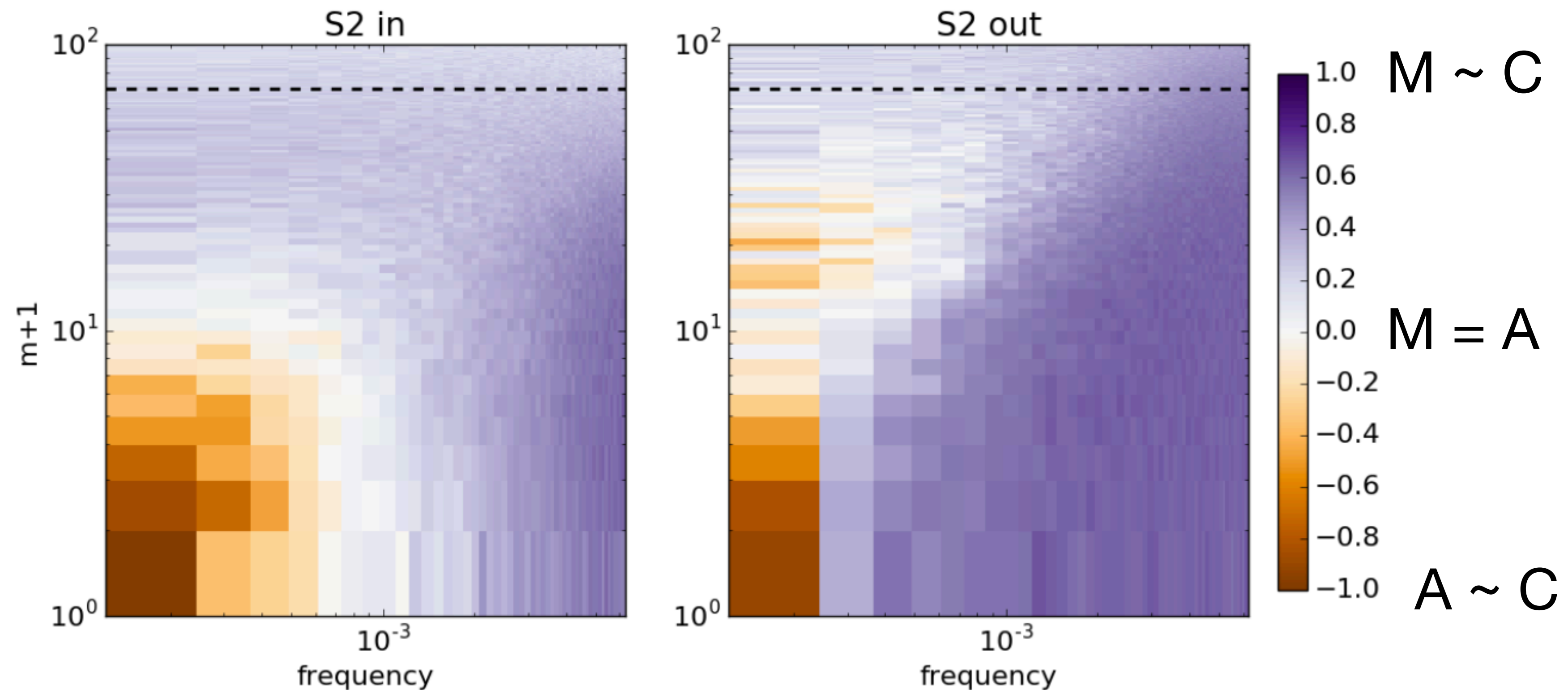


u



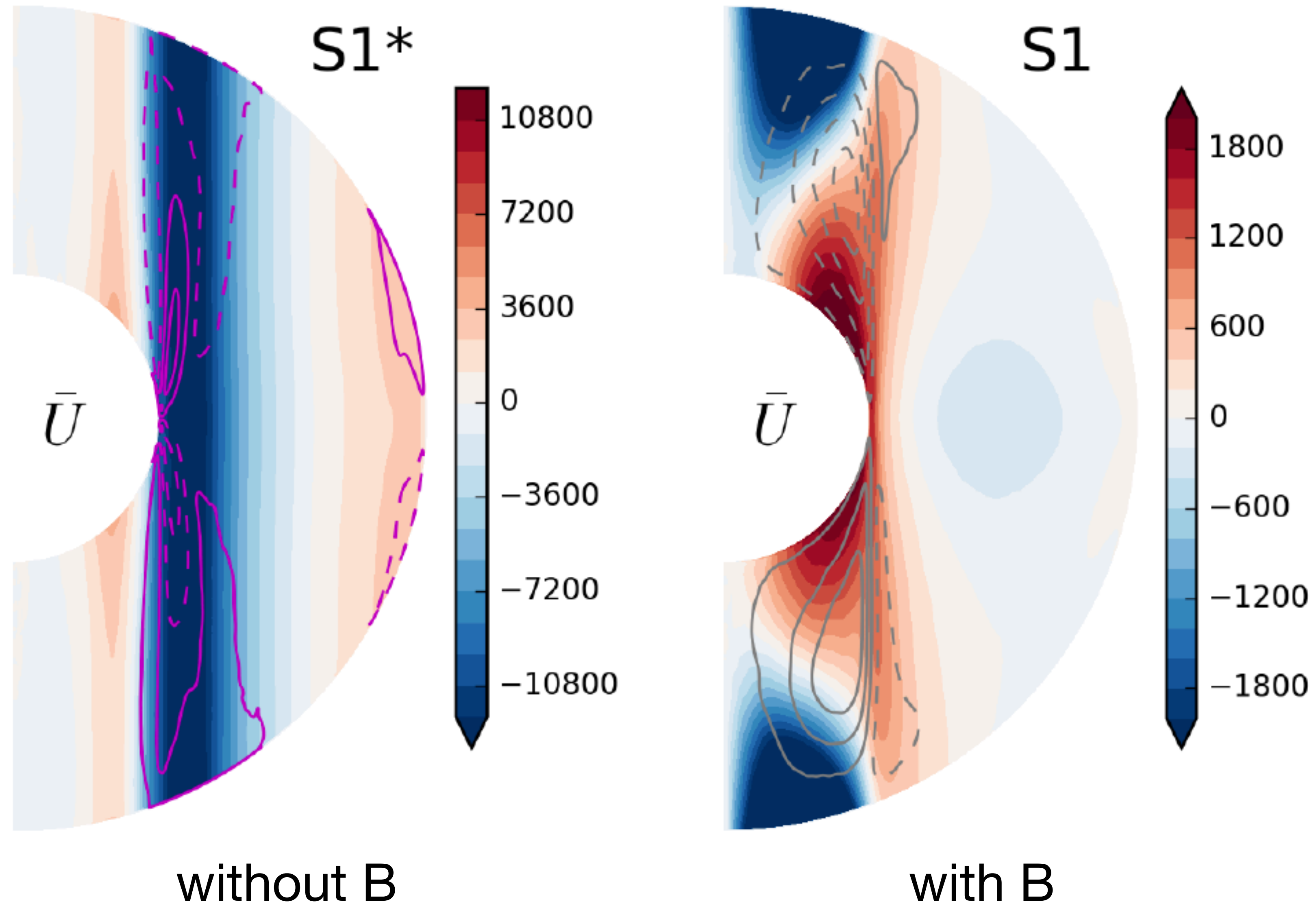
The MAC balance

- The MAC balance is a three term force balance involving Lorentz (M), buoyancy (A), and Coriolis (C) forces. This figure shows $(M-A)/C$ inside (in) and outside (out) the tangent cylinder, as a function of frequency and azimuthal wave number.



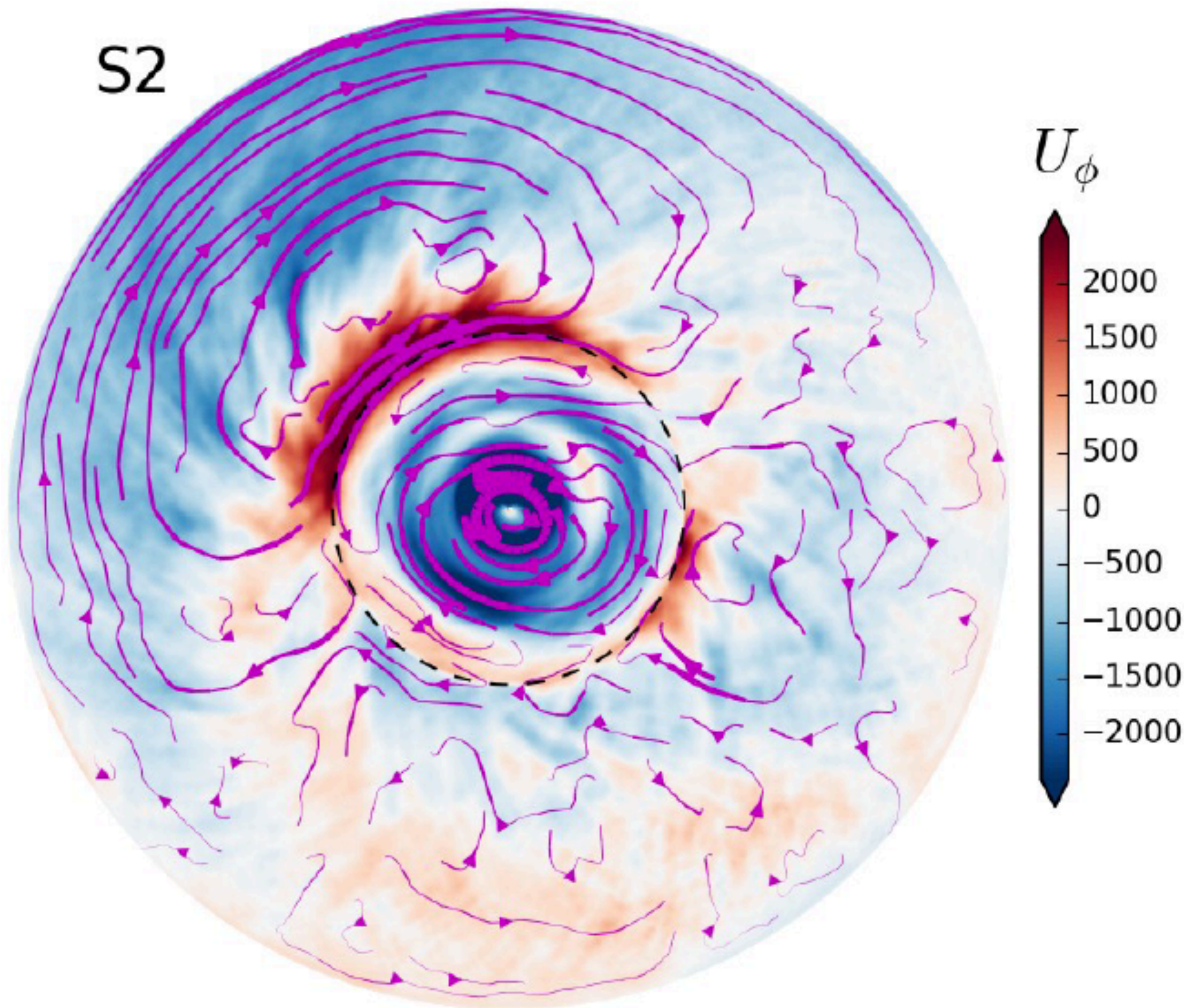
The effect of the magnetic field

- The comparison of dynamo simulation S1 (at $E=10^{-6}$) with the same simulation S1* **without B**, shows the drastic effect of the **magnetic field**, which strongly **inhibits zonal flows** in the outer region, and provokes the apparition of a **huge polar vortex**.
- It also yields a slightly **higher Nusselt** number.



A giant off-centered anti-cyclone...

S2



- The flow averaged over 8 overturn times in simulation S2 ($E=10^{-7}$) reveals a large **off-centered anti-cyclone** in one hemisphere, with little happening in the other hemisphere.
- This is reminiscent of the giant off-centered anti-cyclone retrieved for the core from the inversion of the magnetic secular variation.

Lecture 4

Turbulence in planetary cores

FDEPS

Kyoto, November 29, 2018

4. Turbulence in planetary cores

4.1. What is turbulence?

4.2. Fundamentals of turbulence

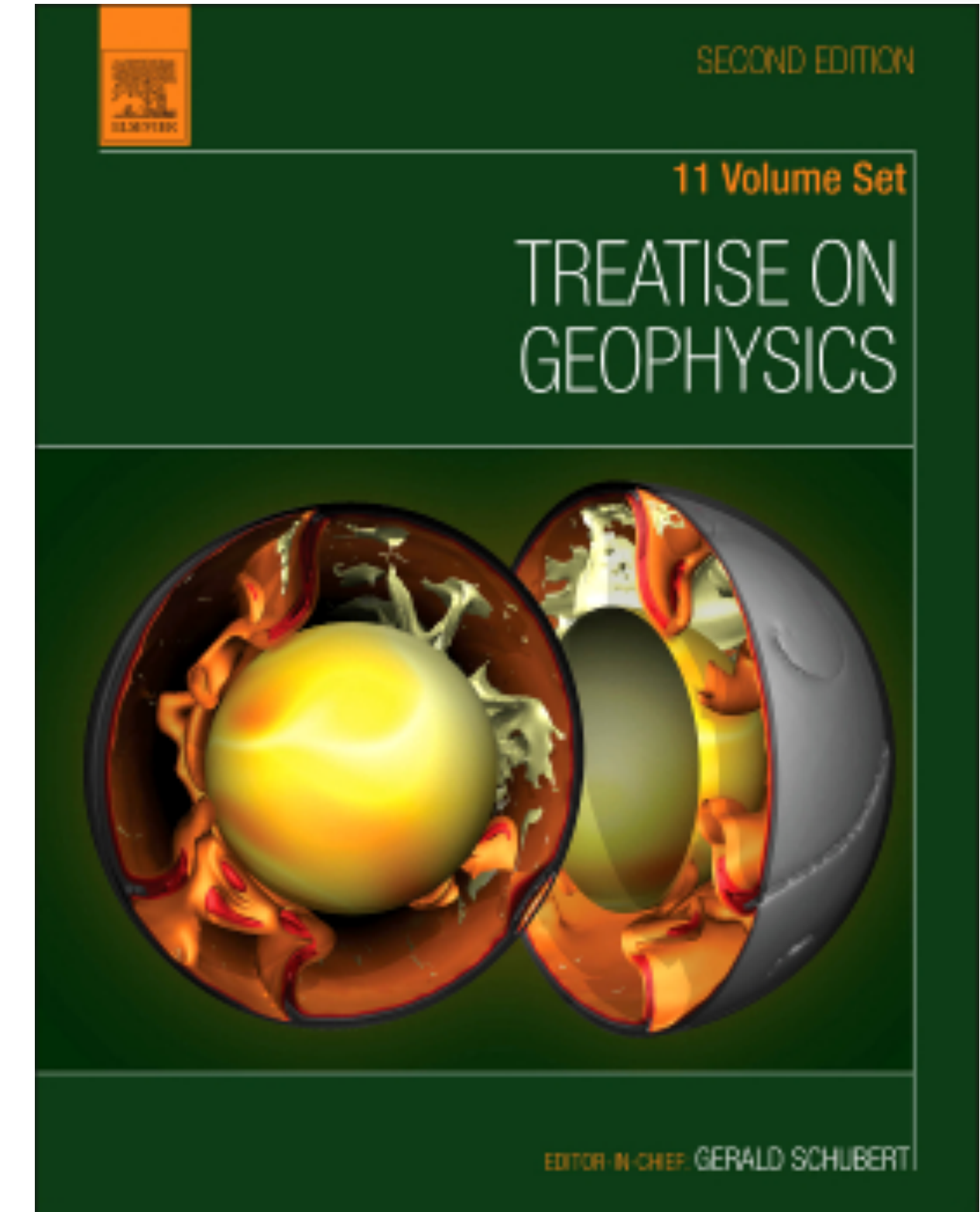
4.3. $\tau - \ell$ regime diagrams

4.3.2. Turbulent convection

4.3.3. Turbulent convection in a rotating sphere

4.3.4. Magnetohydrodynamic turbulence

4.3.5. Turbulence in planetary cores



Nataf & Schaeffer, 2015

4.1. What is turbulence?

clever artistic views...



Leonardo da Vinci
(1452-1519)

*“Big whirls have little whirls that feed
on their velocity, and little whirls have
lesser whirls and so on to viscosity
— in the molecular sense”.*

Lewis Fry Richardson, 1922

4.2. Fundamentals of turbulence

Kolmogorov 1941's universal turbulence



The theory of universal turbulence was established by Kolmogorov (1941). The basic idea is that there should be a wave number k_0 above which turbulence does not depend upon how energy is fed to the flow. The only thing that counts is the mean power per unit mass ε it provides and that is also dissipated in the stationary regime. In this idealized view, universal turbulence should thus be isotropic and homogeneous, and it should have a self-similar character.

The main assumption of Kolmogorov is then that, in the wave number range between the injection wave number k_0 and the dissipation wave number k_D , all statistically averaged quantities at wave number k are a function of k and ε only.

the $k^{-5/3}$ law

The spectral energy density $E(k)$ should thus be a power-law function of ϵ and k only.

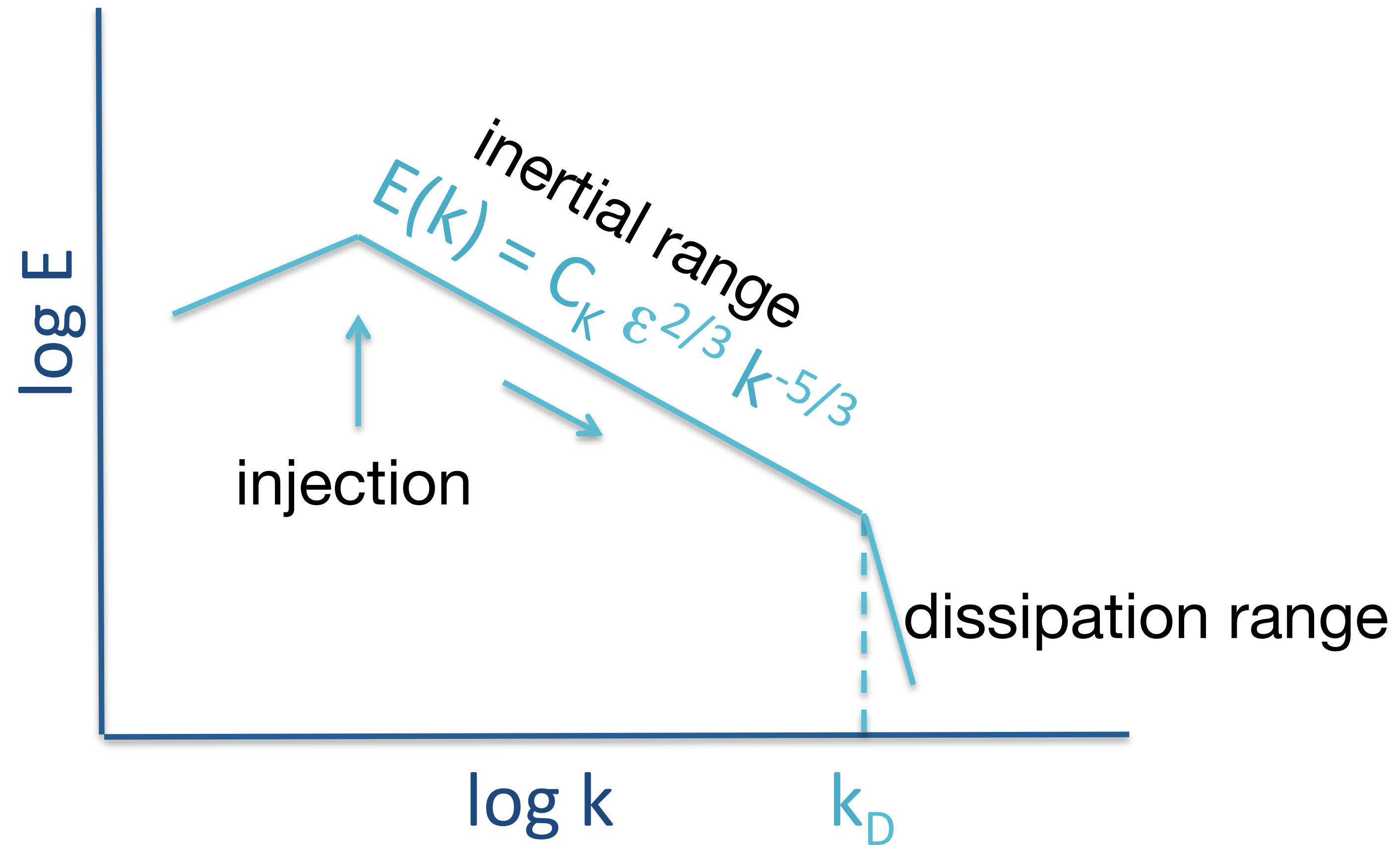
Dimensional analysis: $E(k) \sim \text{m}^3\text{s}^{-2}$, $\epsilon \sim \text{m}^2\text{s}^{-3}$, $k \sim \text{m}^{-1}$

Hence, the famous $k^{-5/3}$ law (derived by Obukhov, 1941):

$$E(k) = C_k \epsilon^{2/3} k^{-5/3}$$

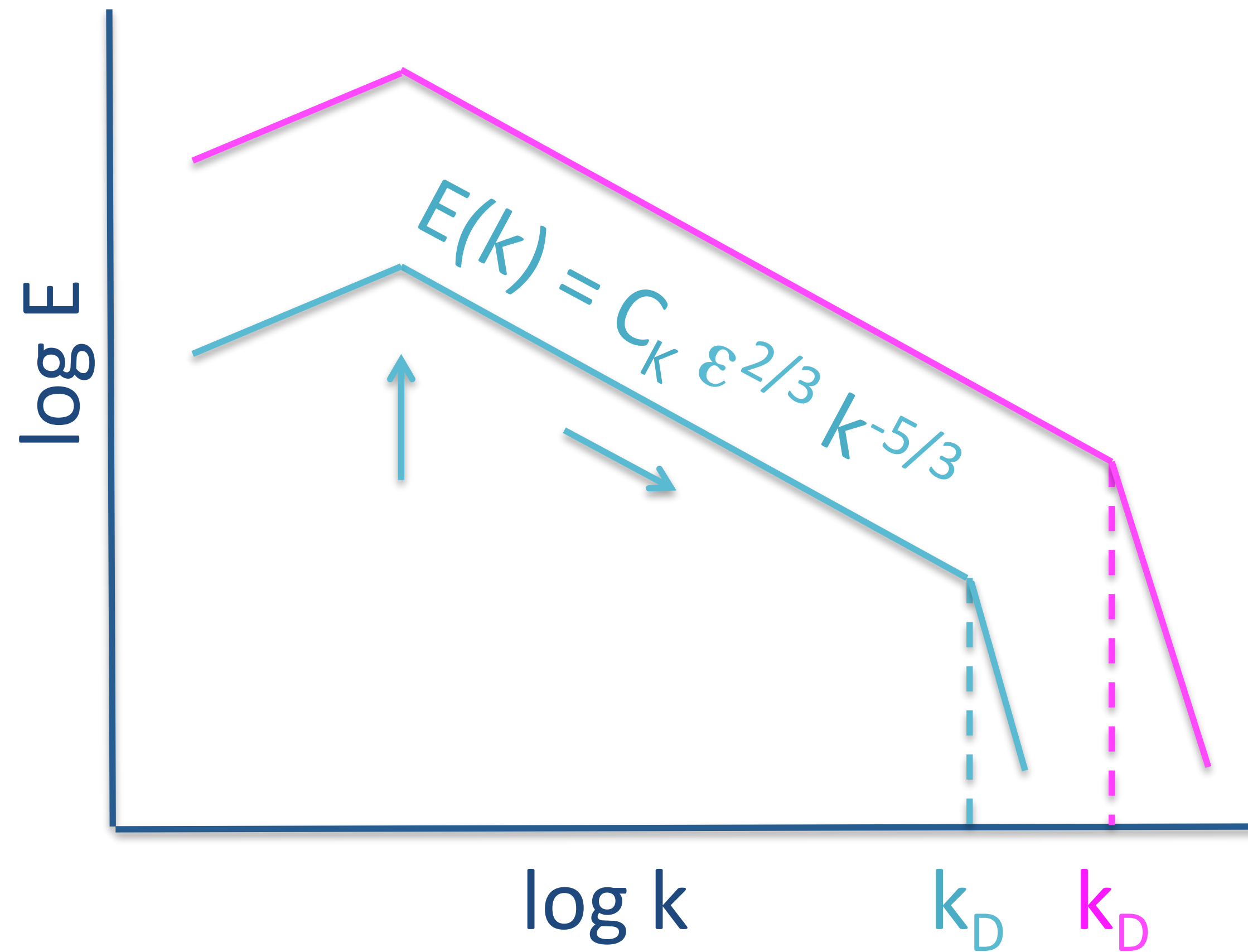
where C_k is the Kolmogorov's constant, which is found to lie between 1.5 and 2.

the turbulent energy cascade



the turbulent energy cascade

and for a larger
power input ε



from k to ℓ

- From now on, we will replace wave number k by a ‘typical’ spatial scale $\ell \sim k^{-1}$ and energy density $E(k)$ by a ‘typical’ time $\tau(\ell) = \ell / U(\ell)$ with $U(\ell) \sim (E(k)k)^{1/2}$

Here, $\tau(\ell)$ is the eddy turnover time.

Note that the $E(k) = C_K \varepsilon^{2/3} k^{-5/3}$ Kolmogorov’s law transforms into:

$$\tau_u(\ell) \sim \ell^{2/3} \varepsilon^{-1/3}$$

the dissipation scale

- The inertial energy cascade reaches the dissipation range at a length scale ℓ_D such that:

* advection balances viscous diffusion, hence the Reynolds number is of order 1 at that scale:

$$Re(\ell_D) = \frac{U(\ell_D)\ell_D}{\nu} \sim 1$$

* viscous dissipation balances the power input, implying: $\nu \frac{U^2(\ell_D)}{\ell_D^2} \sim \epsilon$

- Combining these two relations, we obtain: $\ell_D \sim \left(\frac{\nu^3}{\epsilon} \right)^{1/4}$

different sorts of turbulence

- The amount of literature on *hydrodynamic* turbulence is enormous!
- *Magnetohydrodynamic* turbulence is far from being deciphered.
- Magnetohydrodynamic turbulence in **planetary core conditions** is even less known...
- Let's see what we can guess.

4.3. $\tau - \ell$ regime diagrams

4.3. *tau-ell* regime diagrams

4.3.1. The *tau-ell* recipe

4.3.2. Turbulent Rayleigh-Bénard convection

4.3.3. Turbulent convection in a rotating sphere

4.3.4. Magnetohydrodynamic turbulence

4.3.5. Turbulence in planetary cores

4.3.1. The *tau-ell* recipe

The tau-ell recipe

- Most **dimensionless numbers** can be written as **ratios of typical time scales**.
- For example, using ℓ as a length scale, the Reynolds number can be written as:

$$Re(\ell) = \frac{\tau_\nu(\ell)}{\tau_u(\ell)}$$

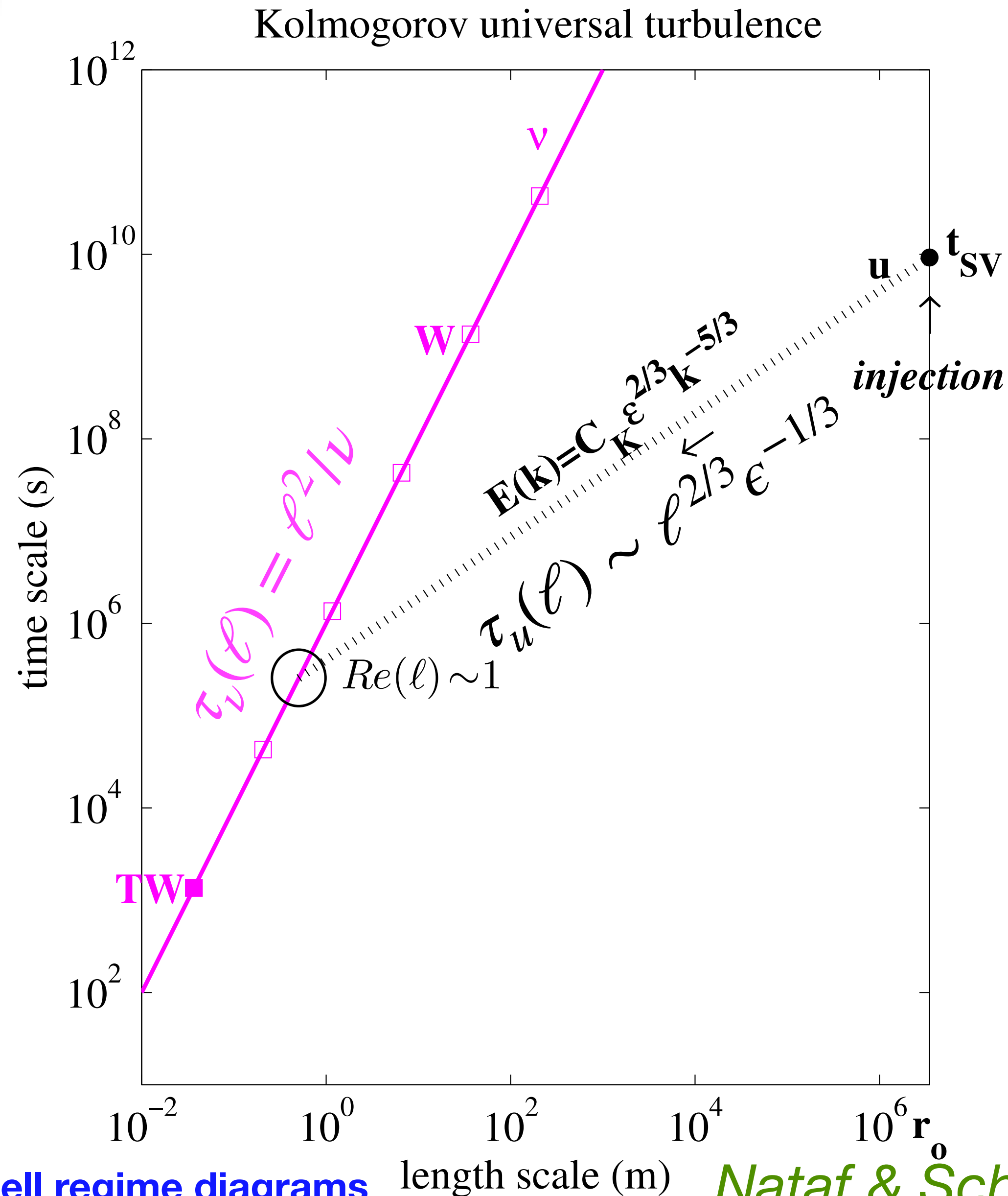
with $\tau_\nu(\ell) = \ell^2/\nu$ the viscous time scale, and $\tau_u(\ell) \sim \ell/U(\ell)$ the eddy turnover time.

The tau-ell recipe

- Dimensionless numbers' values of order 1 mark the transition between different dynamical regimes: from advection to diffusion, for example.
- Therefore, we construct $\tau - \ell$ dynamical regime diagrams by plotting the $\tau(\ell)$ lines of the relevant physical phenomena. The **intersection of these lines mark a dynamical regime change**. They occur for values of an ℓ -scale dimensionless number of order 1.
- For Kolmogorov's turbulence: the lines are the viscous line and the eddy turnover line. The intersection of these two lines defines ℓ_D such that $Re(\ell_D) \sim 1$

Caution: this is a recipe, not a theory...

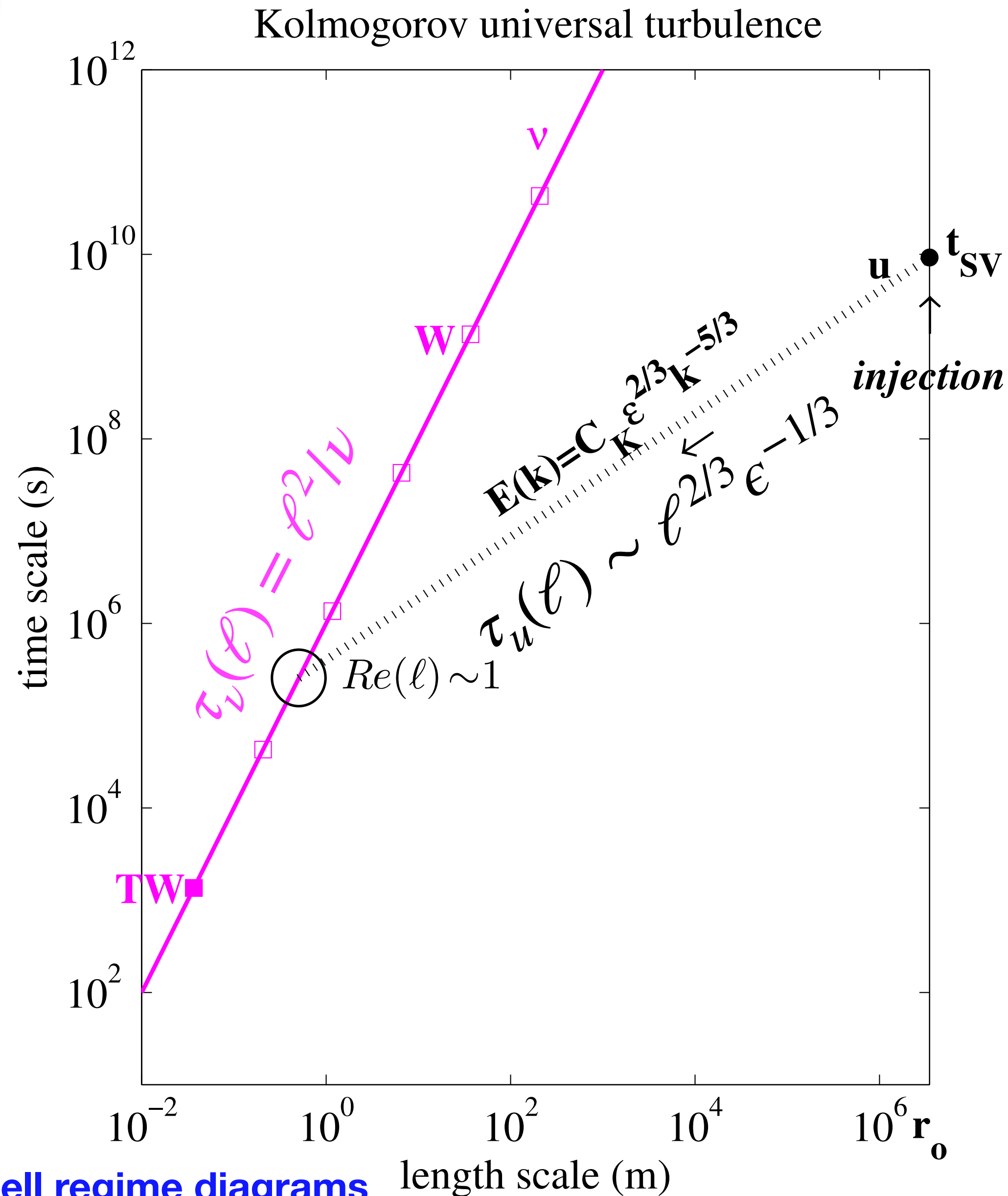
a simple example: Kolmogorov's universal turbulence



We have drawn this example, taking values relevant for the Earth's core:

- maximum length scale:
 $r_o = 3480 \text{ km}$
- kinematic viscosity:
 $\nu \simeq 10^{-6} \text{ m}^2\text{s}^{-1}$
- and we have assumed that the energy injection was at r_o with a typical time equal to the secular variation time:
 $t_{sv} \simeq 300 \text{ years}$

graduating total viscous dissipation



Dissipation occurs where the eddy turnover line hits the viscous line, *i.e.* at length scale $\ell_D \sim \left(\frac{\nu^3}{\epsilon} \right)^{1/4}$

from which we deduce:

$$\epsilon = \nu^3 / \ell_D^4 = \nu / \tau_v^2(\ell_D)$$

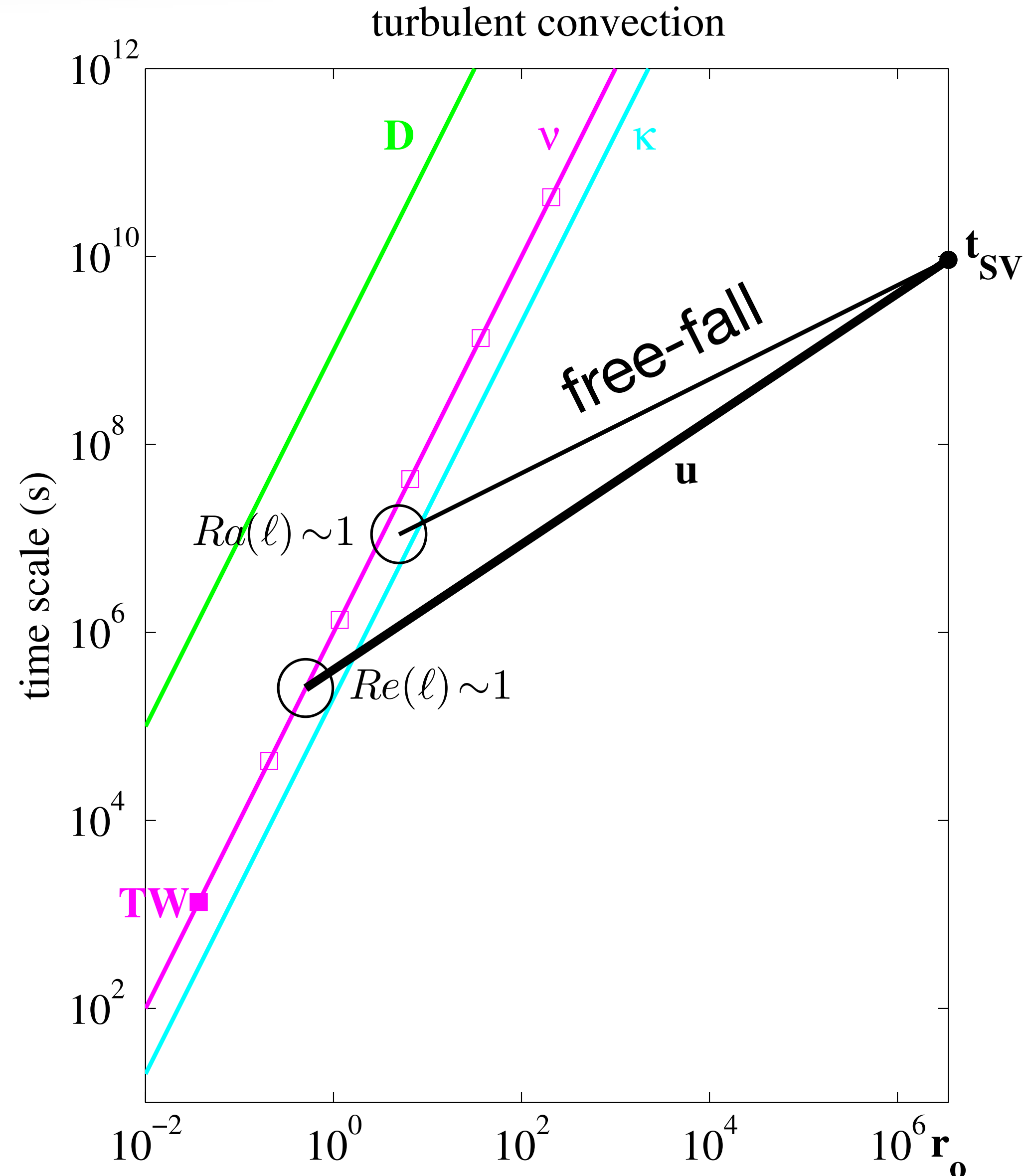
We can thus graduate the viscous line with marks indicating viscous dissipation.

We mark **total viscous dissipation** P_v by multiplying by the mass of the core:

$$M_o = 1.835 \times 10^{24} \text{ kg}$$

4.3.2. Turbulent Rayleigh-Bénard convection

ell-scale times in Rayleigh-Bénard convection



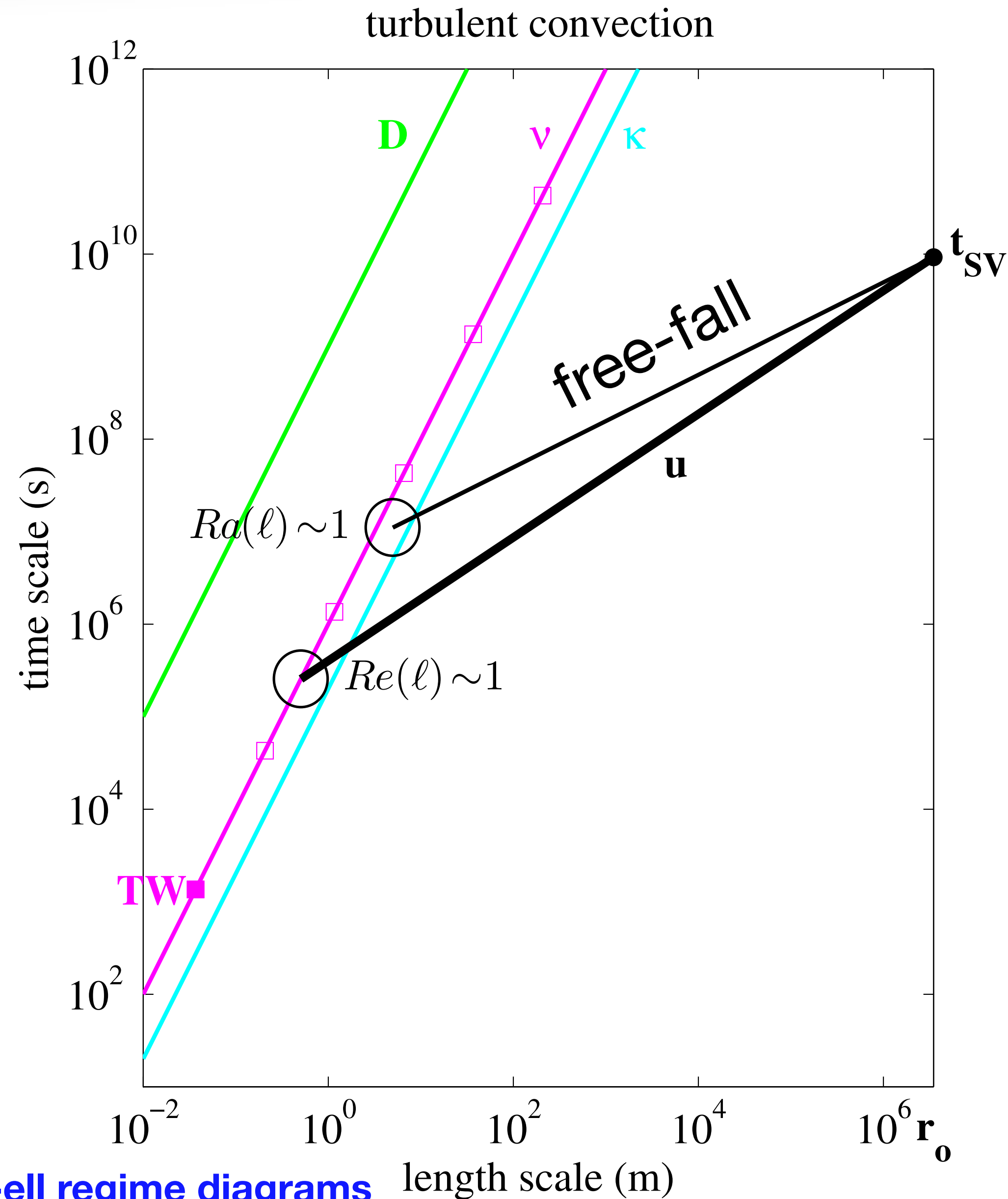
- We have seen that Rayleigh-Bénard started at the system's scale, as an instability powered by the buoyancy force, and braked by two effects: viscous diffusion and thermal diffusion.

- The ℓ scale Rayleigh number can thus be written:
$$Ra(\ell) = \frac{\tau_\kappa(\ell)\tau_\nu(\ell)}{\tau_{FF}^2(\ell)}$$

where τ_{FF} is the buoyancy or free-fall time:

$$\tau_{FF} = \sqrt{\frac{\ell}{g} \frac{\rho}{|\Delta\rho|}}$$

Rayleigh-Bénard convection regime diagram



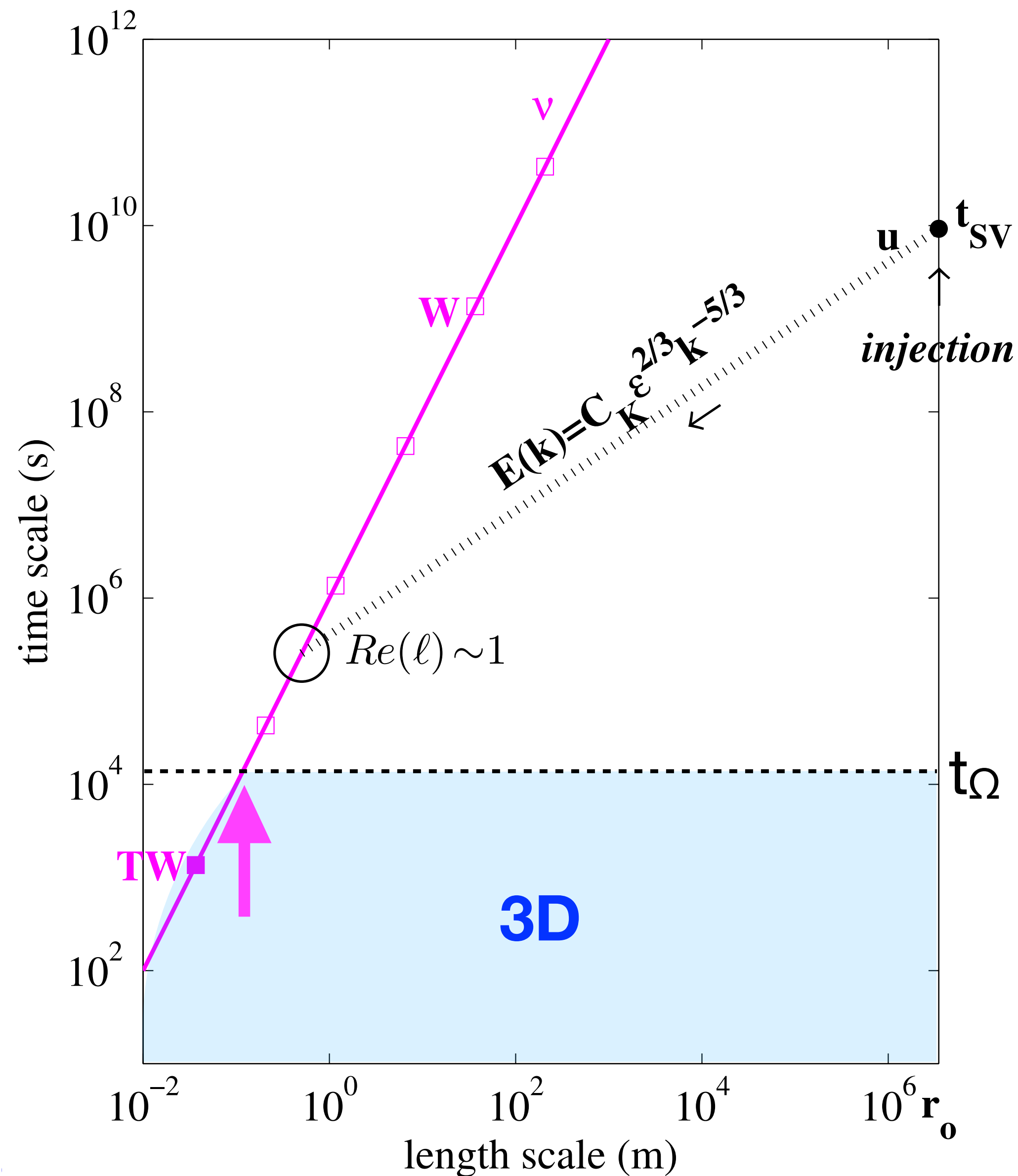
- The smallest convective scale will thus be given by the intersection of the **free-fall line** with the **mid-point between the viscous line and the thermal diffusivity line**.
- Here we have chosen a free-fall time caused by a density contrast $\Delta\rho/\rho$ of only 10^{-15} . It appears to be enough to produce system-scale velocities in the secular variation range. Velocities then cascade down following Kolmogorov's law.

4.3.3. Turbulent convection in a rotating sphere

Questions

- Is there a scale below which turbulence is insensitive to rotation?
- At what scales does thermal convection operate?
- Where is viscous dissipation taking place?

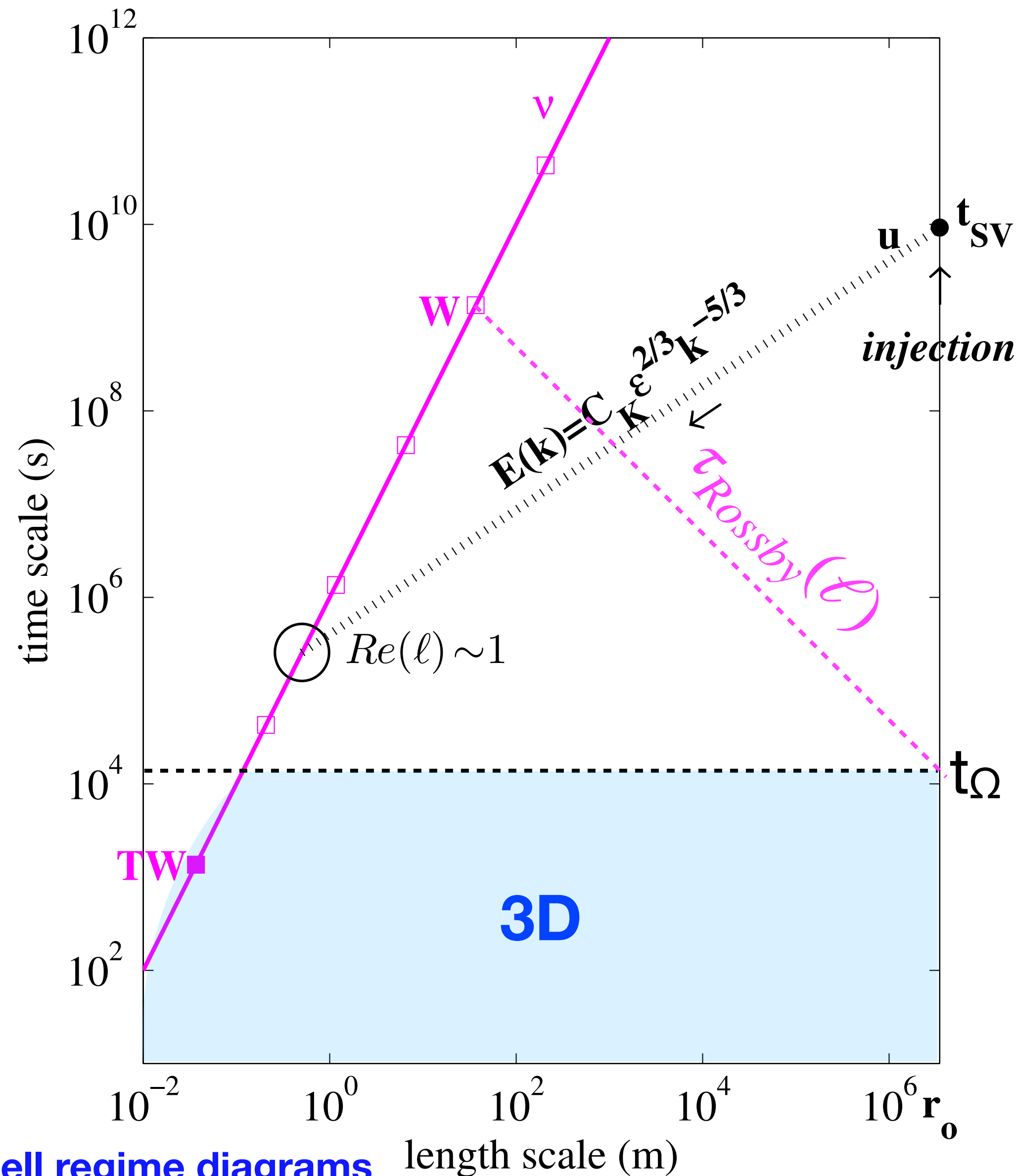
The day line and Ekman layer



- We **add a line** at $t = t_\Omega = \Omega^{-1}$ to our diagram, the '**day**' line.
- Flows at time scale shorter than t_Ω should not be affected by Earth's rotation: this defines the field of **3D** turbulence.
- The intersection of the **viscous line** with the '**day**' line has an ℓ -scale Ekman number $E(\ell) \sim 1$
- It yields the Ekman layer thickness:

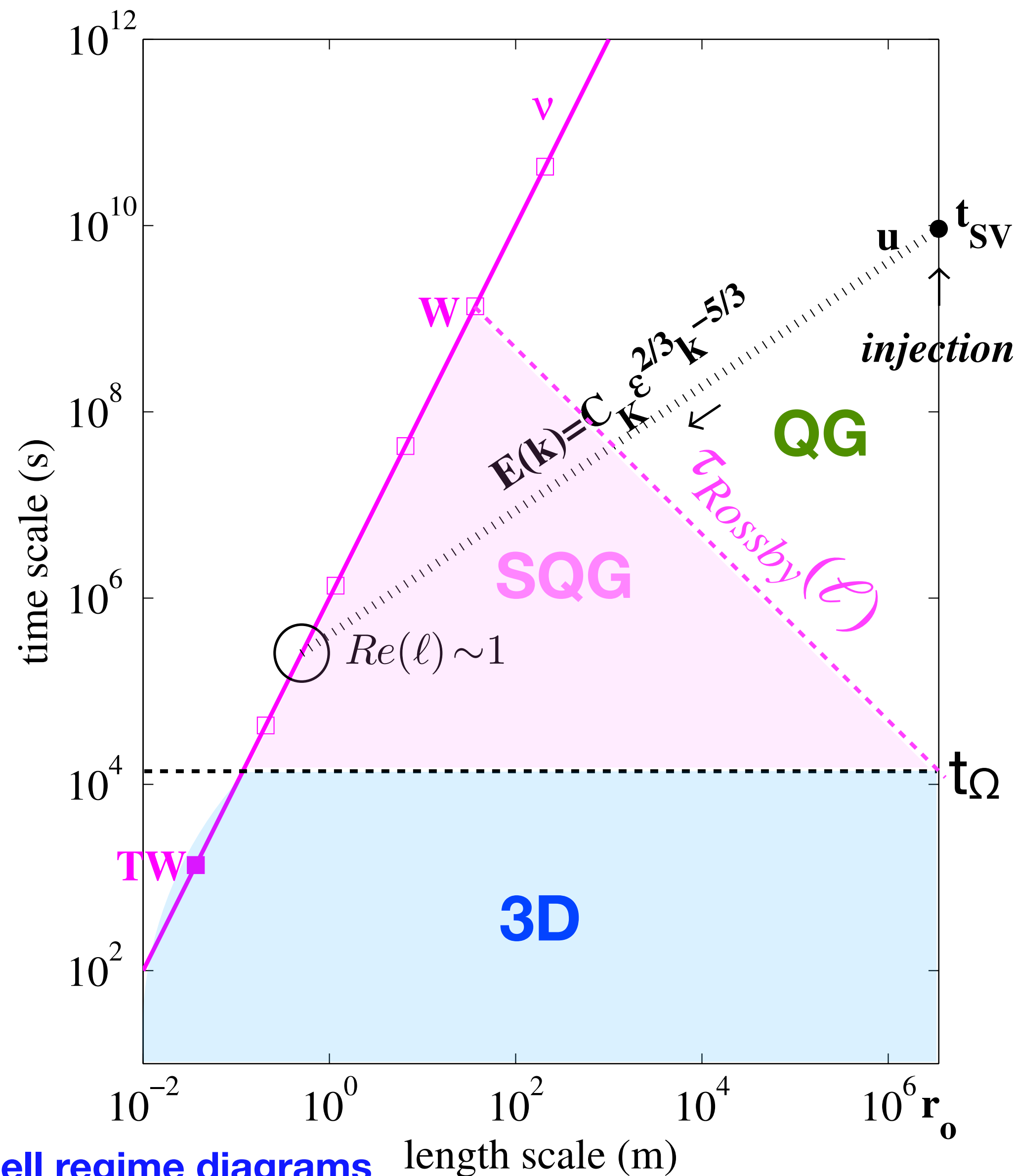
$$\delta_E = \sqrt{\frac{\nu}{\Omega}} \simeq 10 \text{ cm}$$

The Rossby line



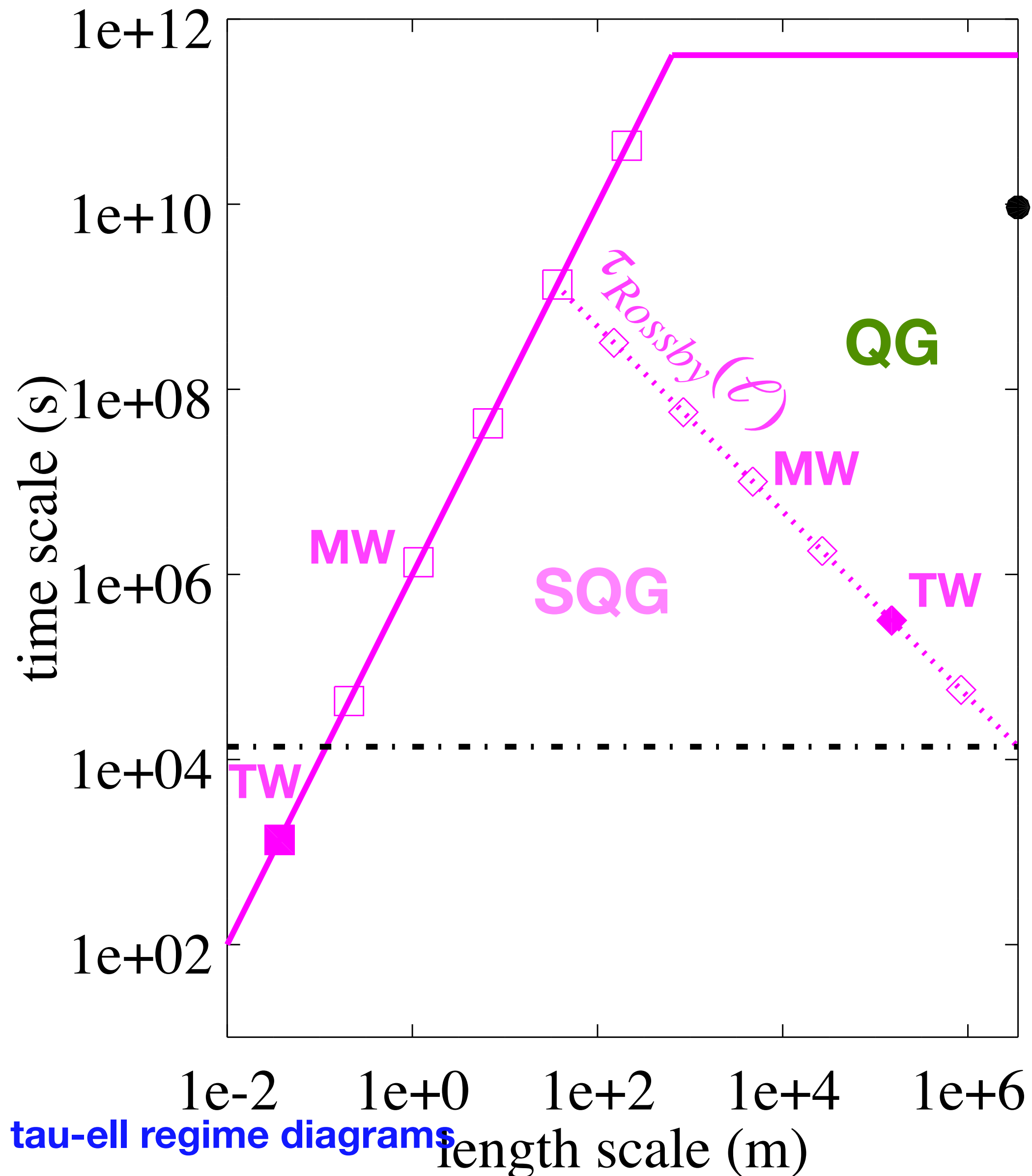
- We add a second line: the **Rossby line**, defined by: $\tau_{Rossby}(\ell) = \frac{r_0}{\Omega \ell}$
- This line describes two phenomena:
 - the time it takes for a **Rossby wave to propagate** one wave length ℓ .
 - The time it takes for a patch of diameter ℓ to form a complete Taylor column across the core.

Quasigeostrophic and semi-quasigeostrophic turbulence



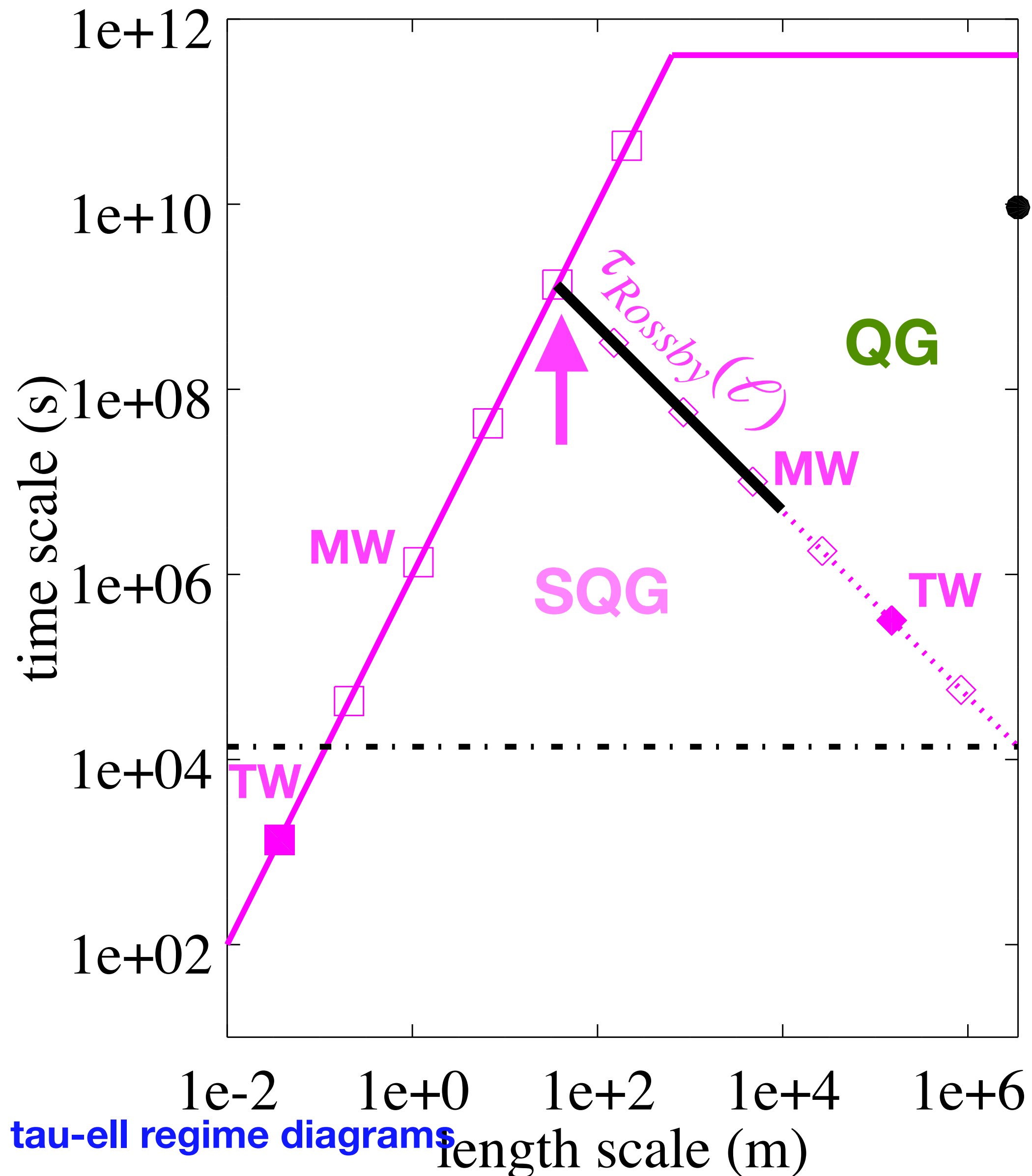
- Flows that habit the **triangle** formed by the ‘**day**’ line, the **Rossby line**, and the **viscous line** will feel the rotation of the Earth and form **elongated** structures, but won’t have time to form complete Taylor columns, producing **semi-quasigeostrophic (SQG)** turbulence.
- Above the Rossby line, we expect **quasigeostrophic (QG)** flows.

QG dissipation



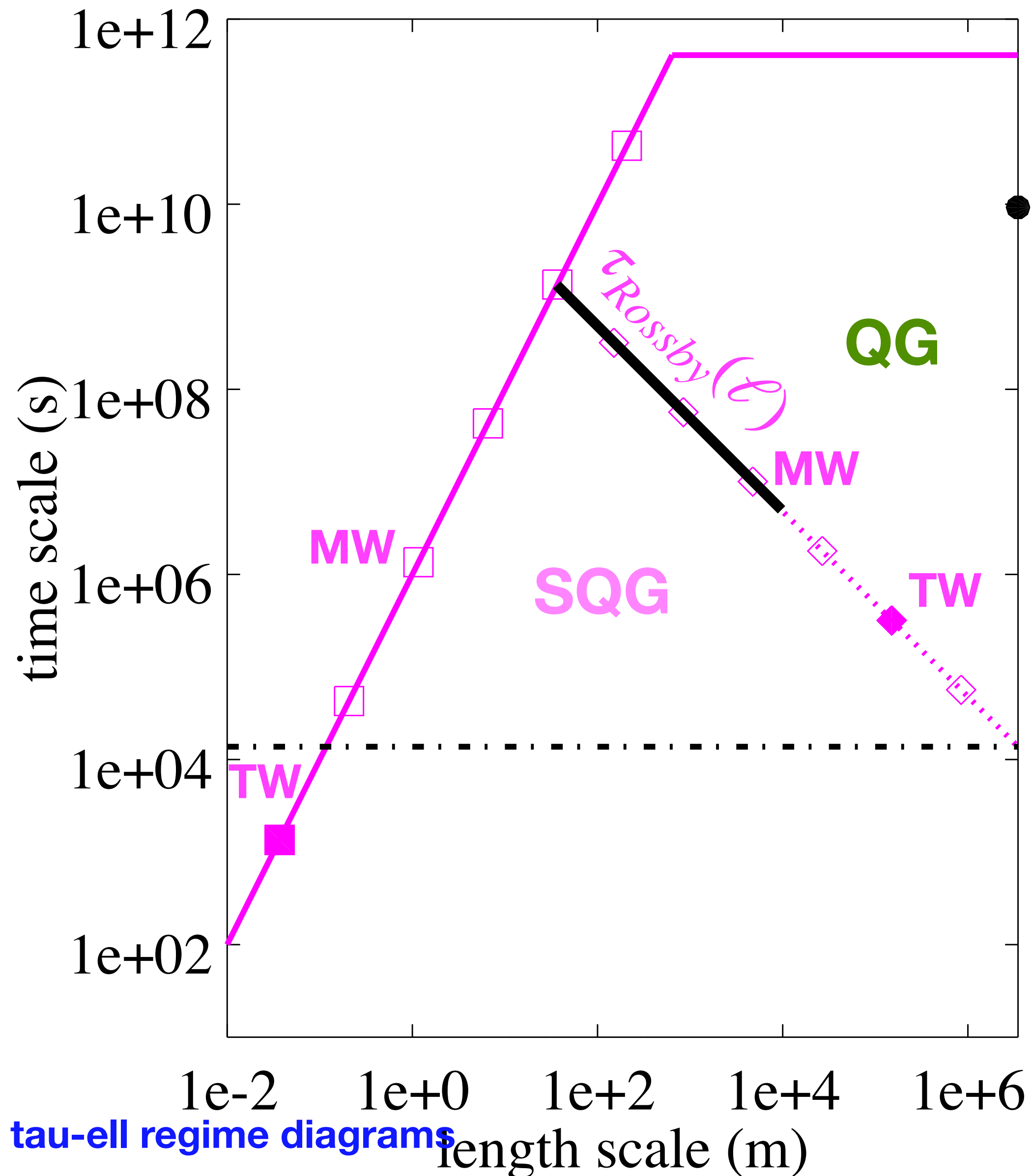
- The **viscous dissipation** of quasigeostrophic flows occurs in the **Ekman layers** at both ends of the columns. We **graduate the Rossby line** with the corresponding total dissipation.

QG convection

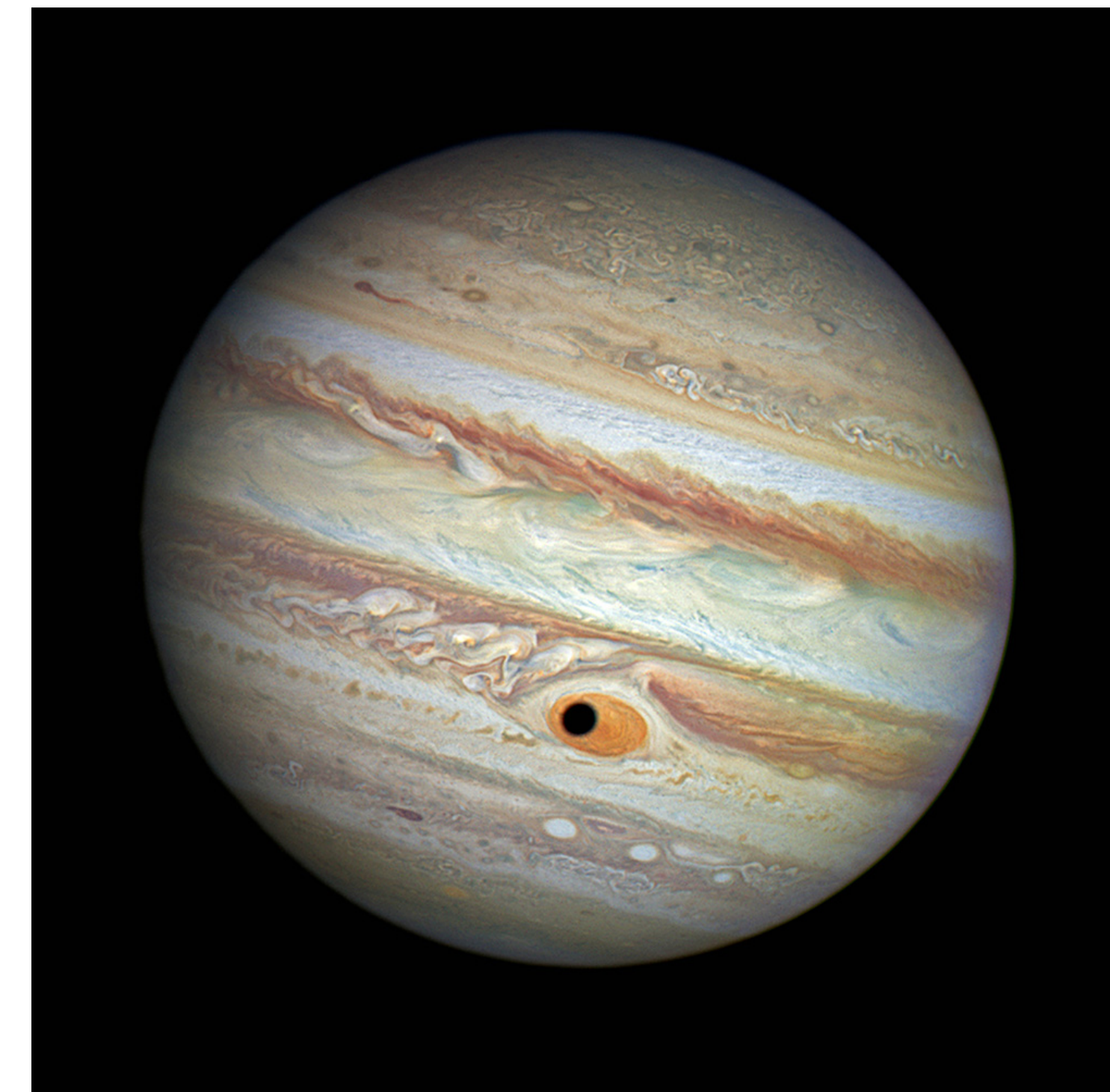


- In contrast to Rayleigh-Bénard convection, we have seen that thermal convection is **small-scale** at the threshold, taking the form of a **viscously controlled Rossby wave**.
- The onset will thus be at the ℓ scale and τ scale at the intersection of the **viscous line** and the **Rossby line**. As the forcing increases, the flow will follow an **inverse cascade along the Rossby line** (Guervilly et al, 2018).

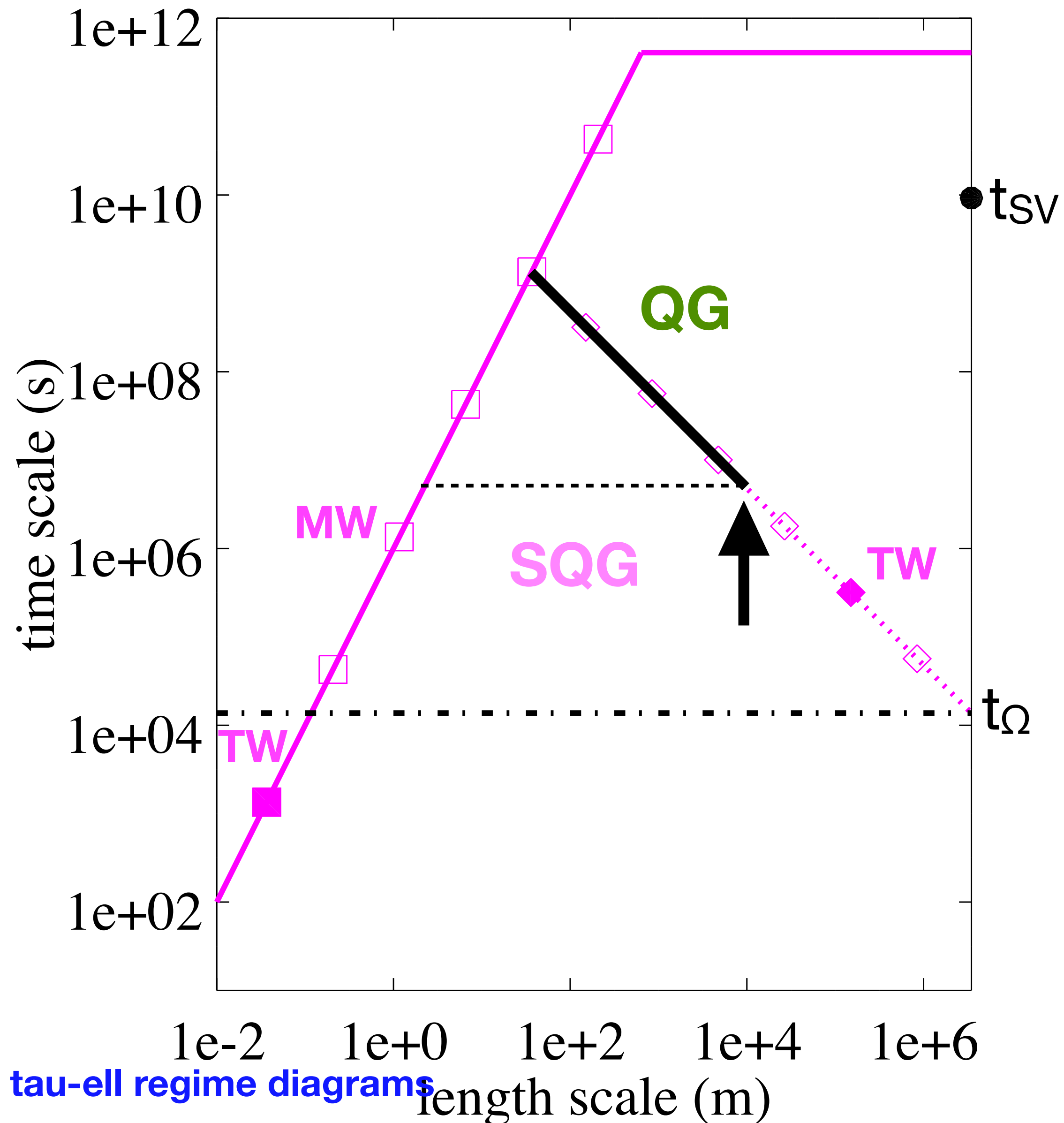
QG convection



- Non-linear interactions of these Rossby wave eddies drive **azimuthal flows**. The inverse cascade stops where the eddies reach the **Rhines scale**.



Inverse cascade and the Rhines scale



- The Rhines scale is given by:

$$\ell_{Rhines} = \sqrt{\frac{u_{\phi} r_o}{\Omega}} = \sqrt{\frac{2\pi r_o}{t_{sv}} \frac{r_o}{\Omega}} \simeq r_o \sqrt{\frac{t_{\Omega}}{t_{sv}}} \sim 10 \text{ km}$$

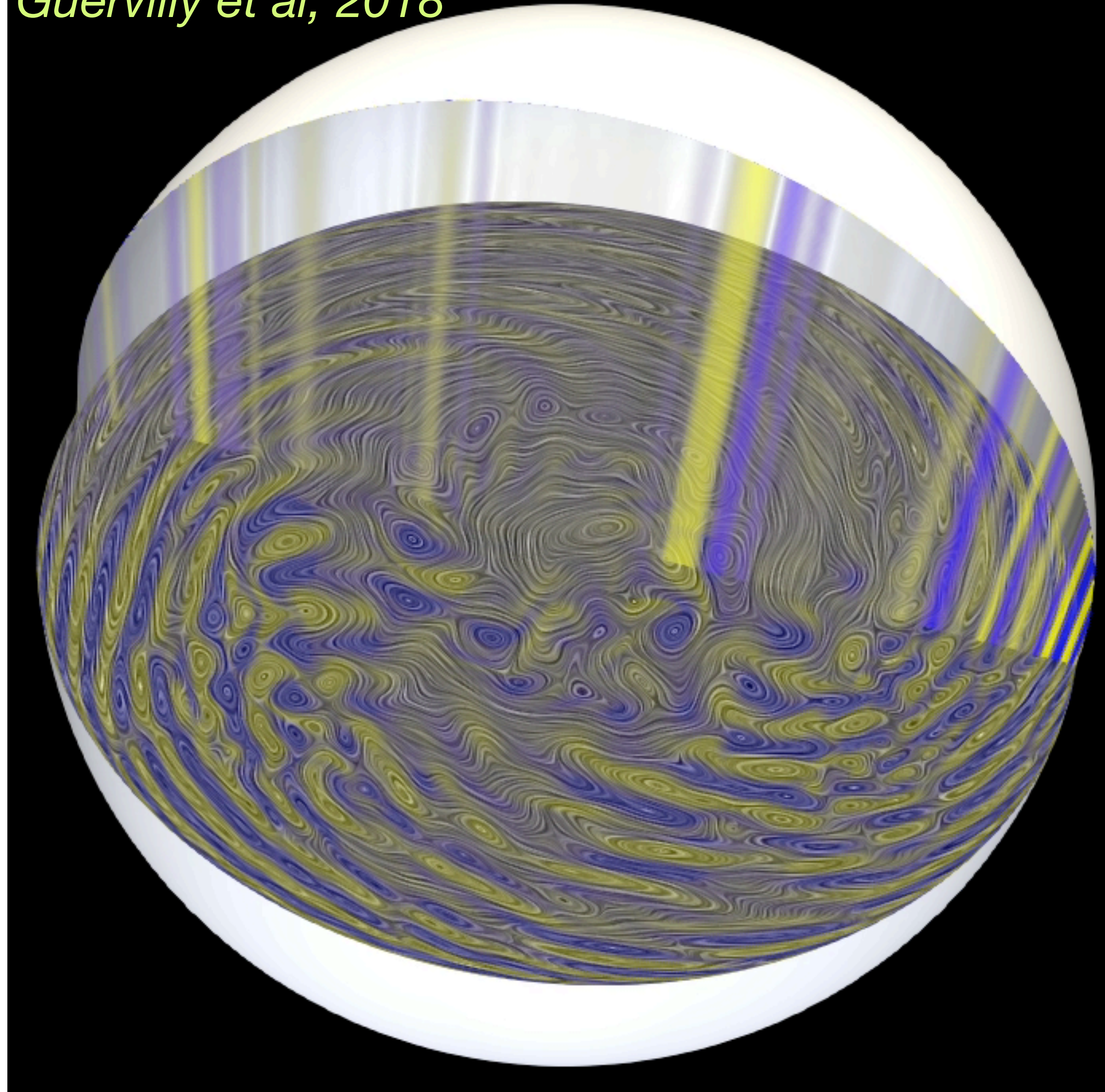
where we have reinterpreted the secular variation time t_{sv} as the time it takes for an **azimuthal jet to circle around the planet**.

- Note that viscous dissipation is maximum at that scale, and is dominated by **dissipation in the Ekman layers** (Guervilly et al, 2018).

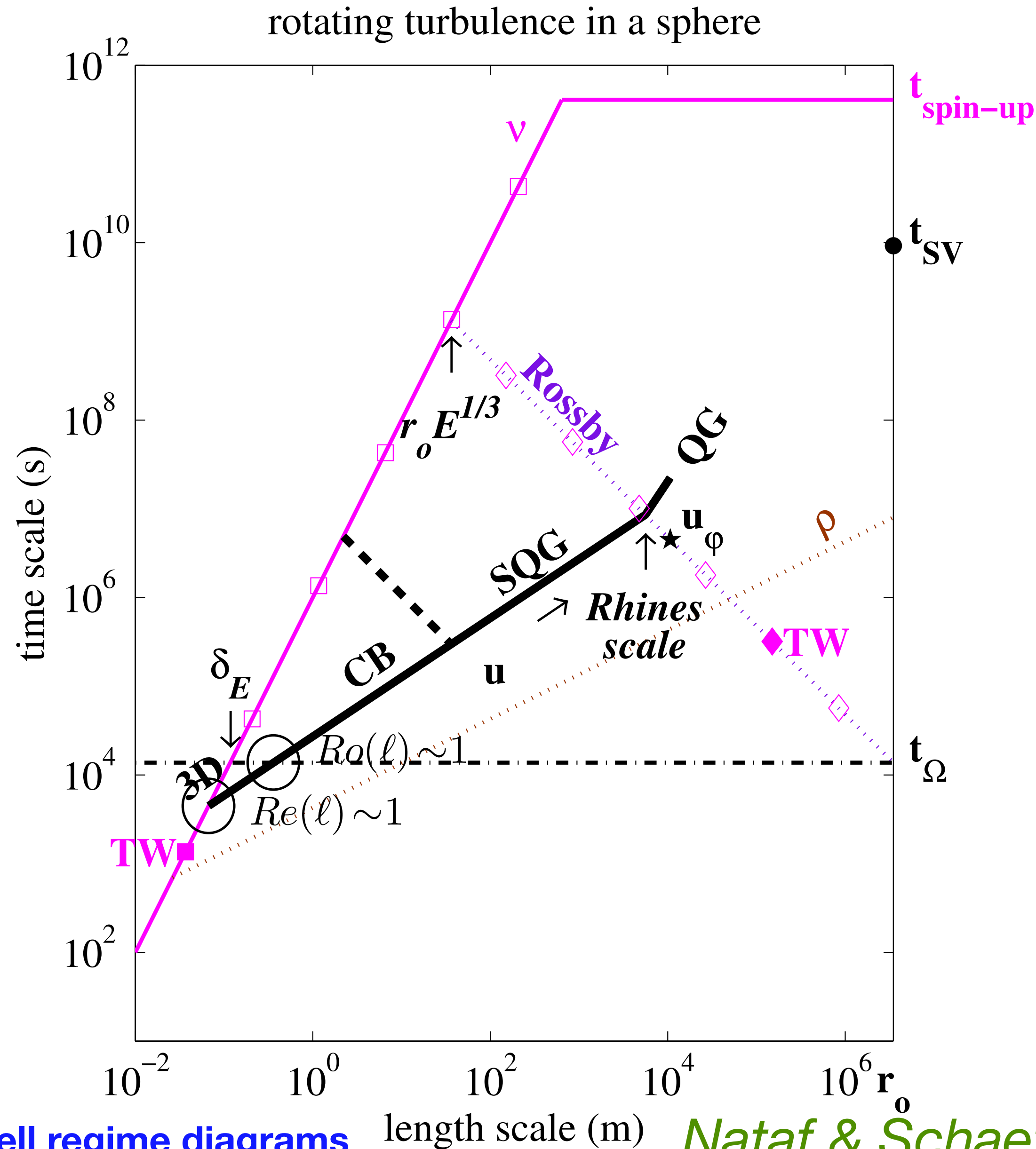
- It could be that the energy is injected directly at the Rhines scale, and cascades down to the small-scales.
- Note that in this scenario, turbulence never gets 3D, nor even semi-quasi-geostrophic.

Vorticity (colors) and streamlines in a 3D numerical simulation of thermal convection at $E = 10^{-7}$, $Ra = 7 \cdot 10^8$, $Pr = 10^{-2}$.

Guervilly et al, 2018



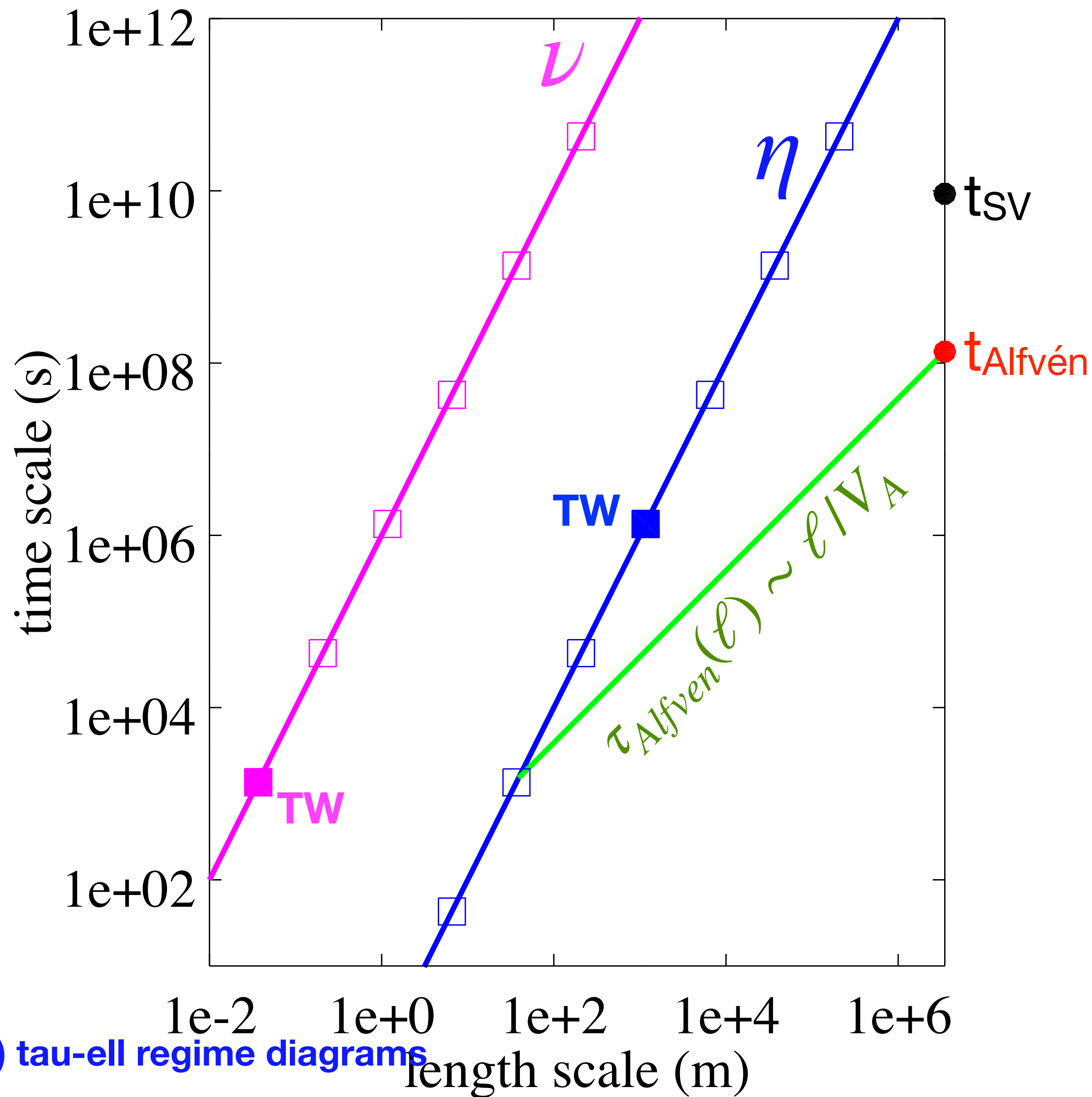
ToG correction...



- In the *Treatise on Geophysics* (2015), we had proposed this very different scenario. It also rested on a balance between eddies and inertial waves, but we had wrongly taken the **critical balance of unconfined inertial waves** (Nazarenko & Schekochihin, 2011) **ignoring** the fundamental role of the **spherical boundaries**.

4.3.4. Magneto hydrodynamic turbulence

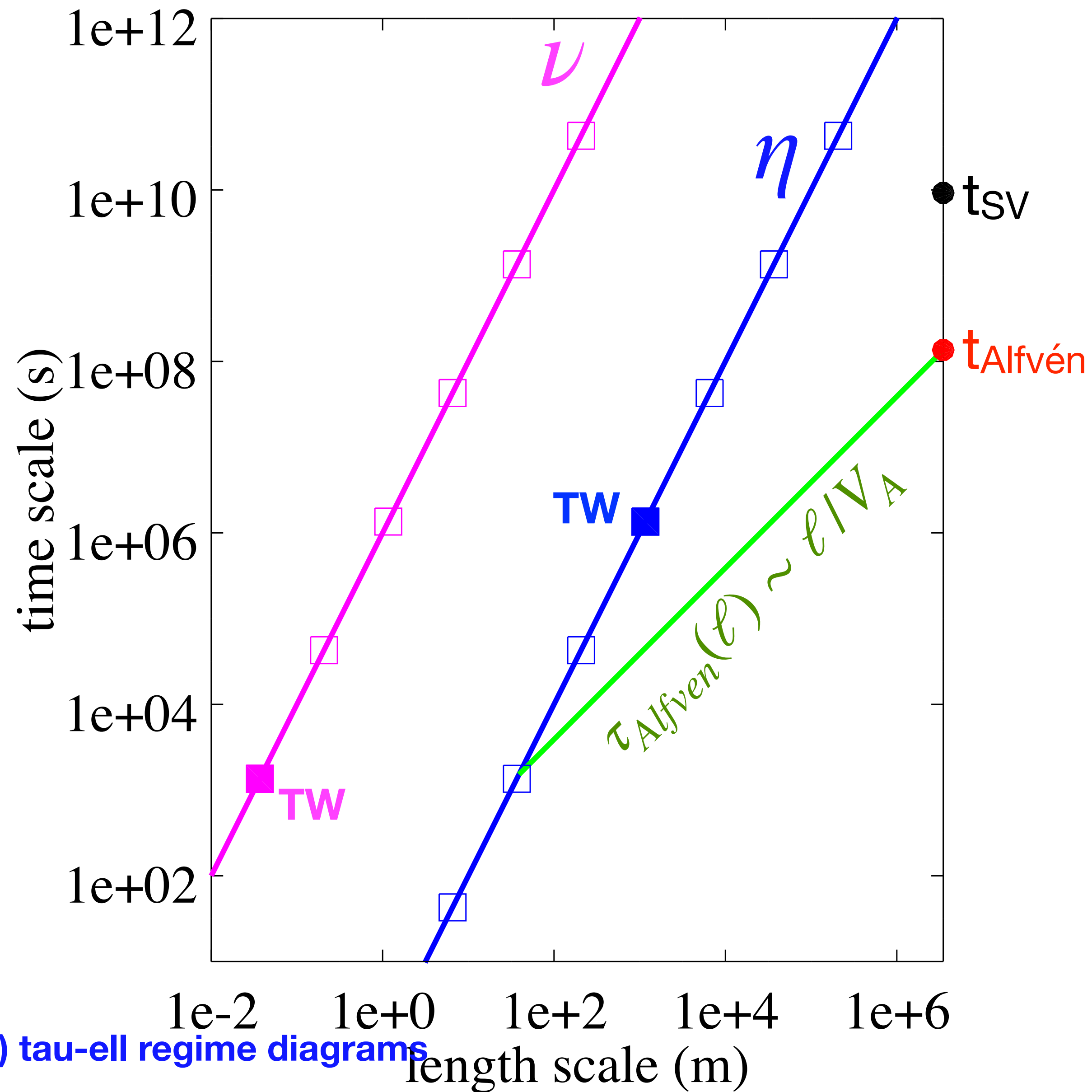
Magnetic diffusion and Alfvén waves



- We ignore rotation for the moment, and add the magnetic field, which we assume to be large-scale dominated.
- From the observation of torsional Alfvén waves in the core (Gillet et al, 2010), we get a **characteristic time** $t_{\text{Alfvén}} = 4 \text{ years}$.
- Magnetic diffusion is much larger than viscous diffusion, since the magnetic Prandtl number in the core is:

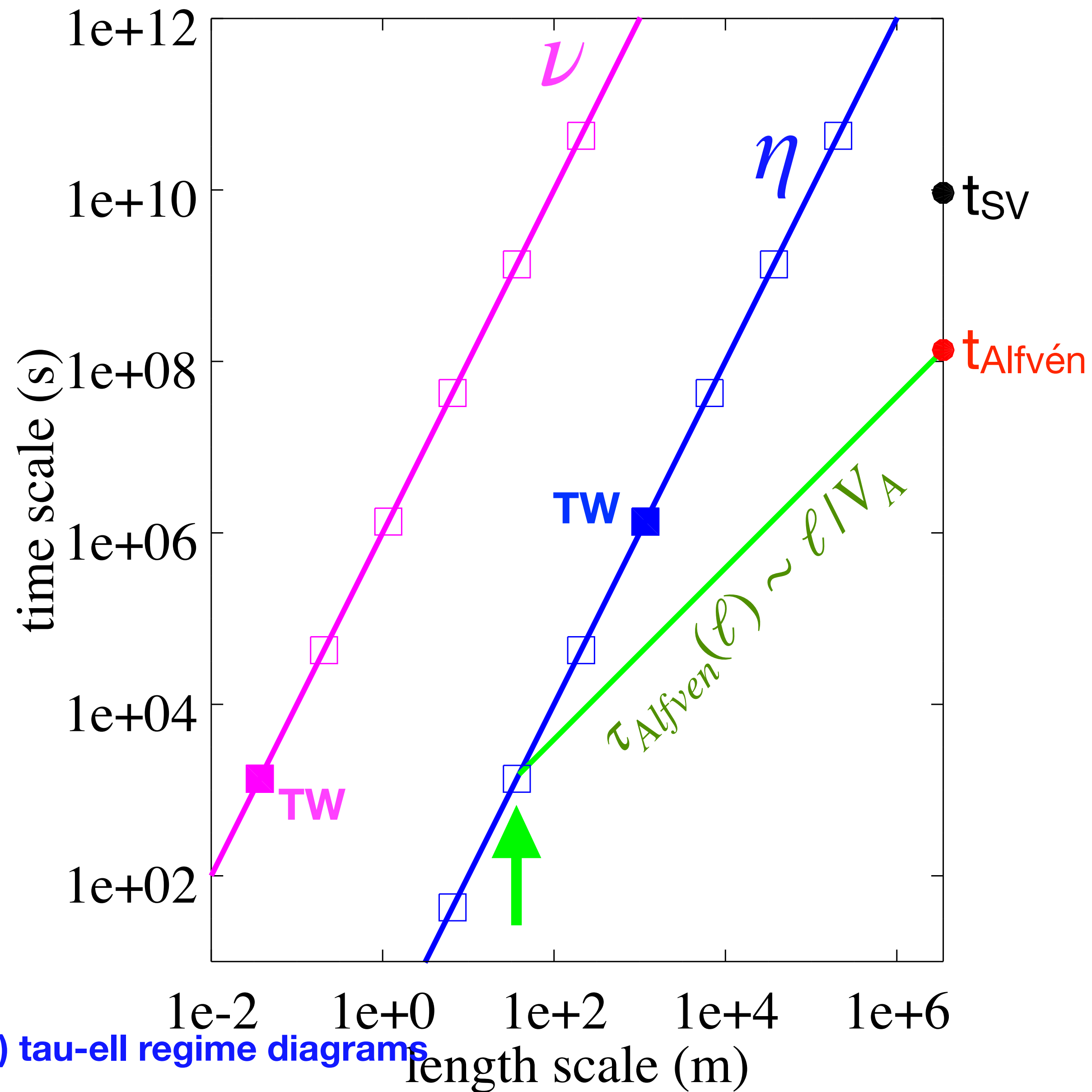
$$Pm = \frac{\nu}{\eta} \simeq 10^{-6}$$

Magnetic diffusion and Alfvén waves



- We add the **magnetic diffusion line**, and an **Alfvén wave line**, defined by the time it takes for an Alfvén wave to travel a distance ℓ (assuming the Alfvén wave speed is that of the large-scale magnetic field).
- The Alfvén time plays a role equivalent to the eddy turnover time for the flow. It characterizes the magnetic energy at the considered scale, and we want to build the plausible $\tau_b(\ell)$ and $\tau_u(\ell)$ lines for MHD turbulence.

The Lundquist number



- The **Lundquist number** compares the magnetic diffusion time to the Alfvén wave propagation time:

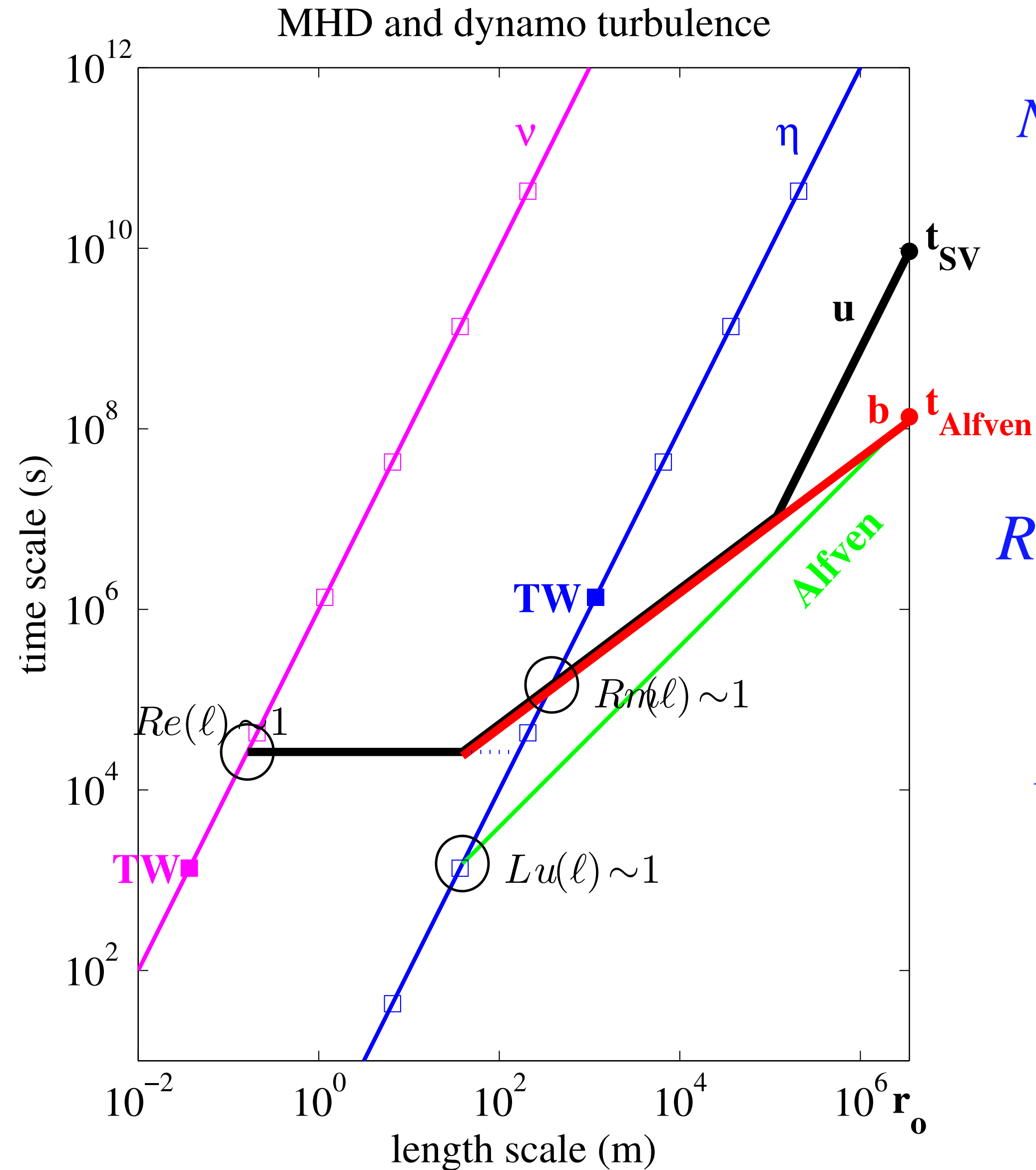
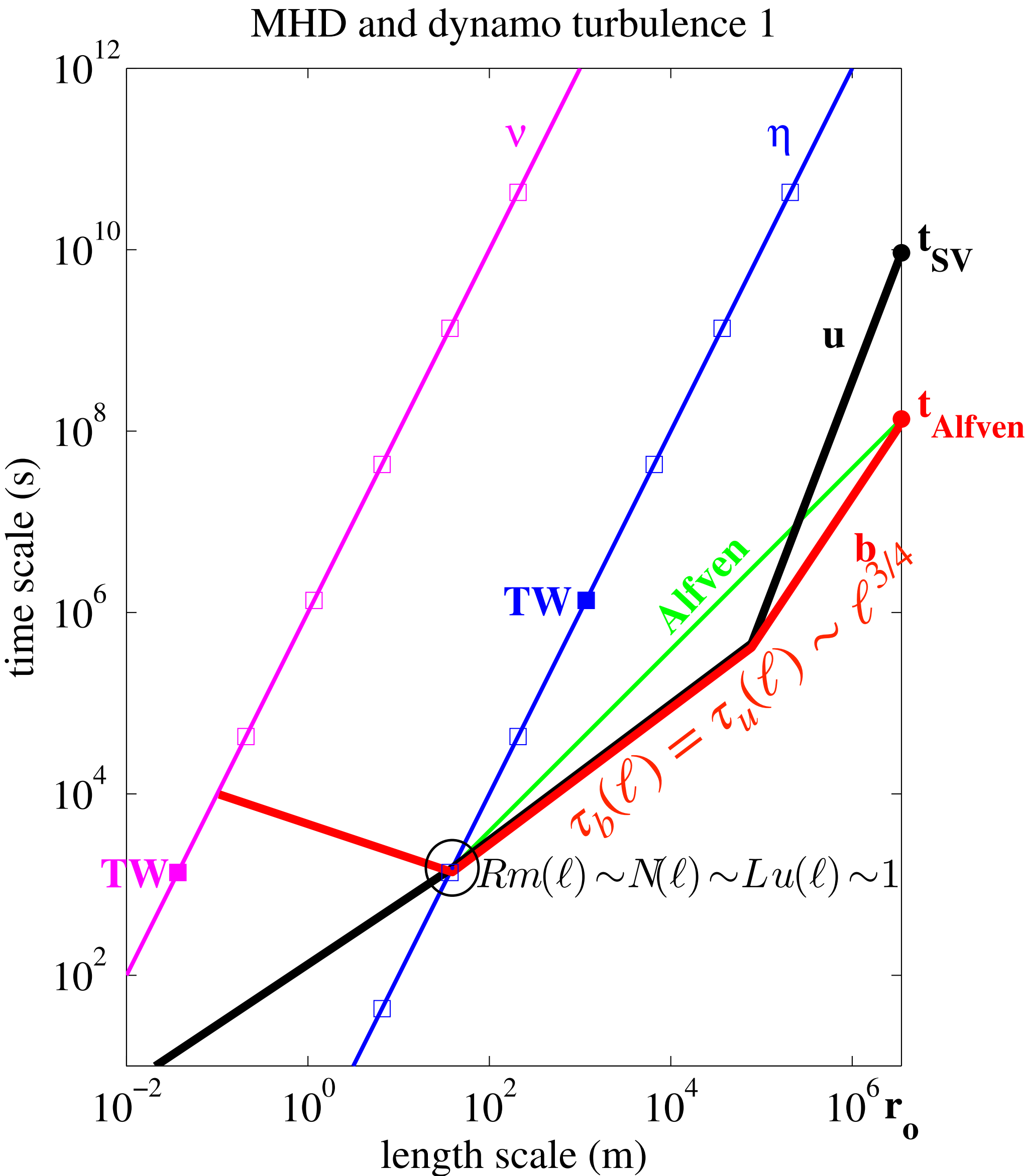
$$Lu(\ell) = \frac{\tau_{\eta}(\ell)}{\tau_{\text{Alfvén}}(\ell)}$$

- It is of order one at the intersection of the **magnetic diffusion line** with the **Alfvén wave line**. At smaller length scales, Alfvén waves cannot propagate anymore.

MHD turbulence

- It is believed that MHD turbulence is controlled by the **collision of Alfvén waves**, which cascade the energies from large scale to small scale (e.g., Tobias et al, 2013).
- In Alfvén waves, energy is **equally** partitioned between **magnetic** and **kinetic** energy.
- Two regimes are identified, yielding different cascade exponents: **weak** collisions and **strong** collisions ($E(k) \sim k^{-3/2}$).
- We built two possible scenarios, which I briefly discuss, keeping in mind they are very speculative, but raise some interesting issues.

2 scenarios of MHD turbulence



$$N(\ell) = \frac{\tau_u^2(\ell)}{\tau_{Alfven}(\ell)\tau_b(\ell)}$$

$$Rm(\ell) = \frac{\tau_\eta(\ell)}{\tau_u(\ell)}$$

$$Lu(\ell) = \frac{\tau_\eta(\ell)}{\tau_{Alfven}(\ell)}$$

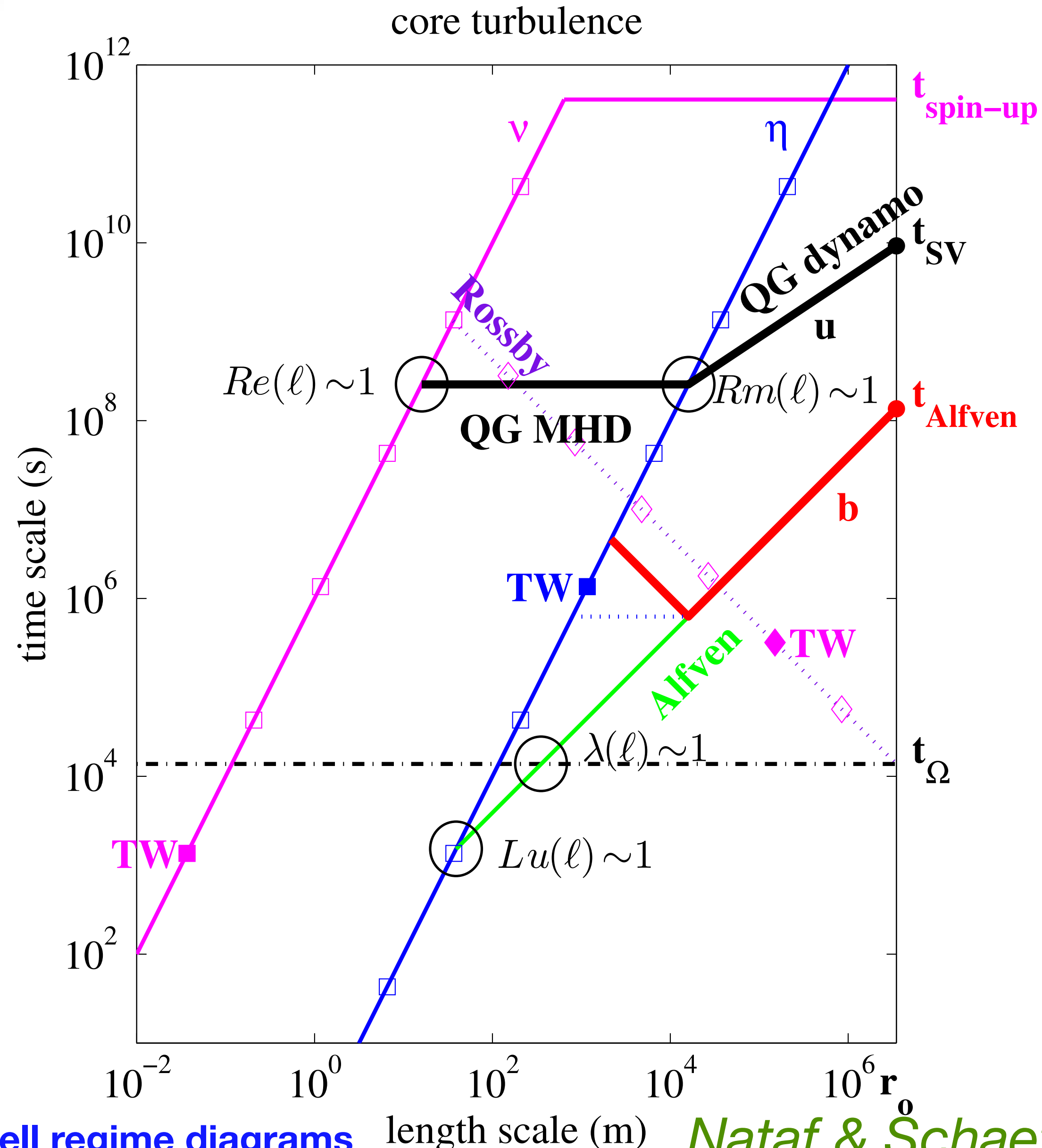
Too large dissipation

- Note that both scenarios come up with **magnetic dissipation** much larger than the total heat that gets out of the Earth. The Earth would not be able to produce a magnetic field of its current intensity if it were not rotating.

4.3.5. Turbulence in planetary cores

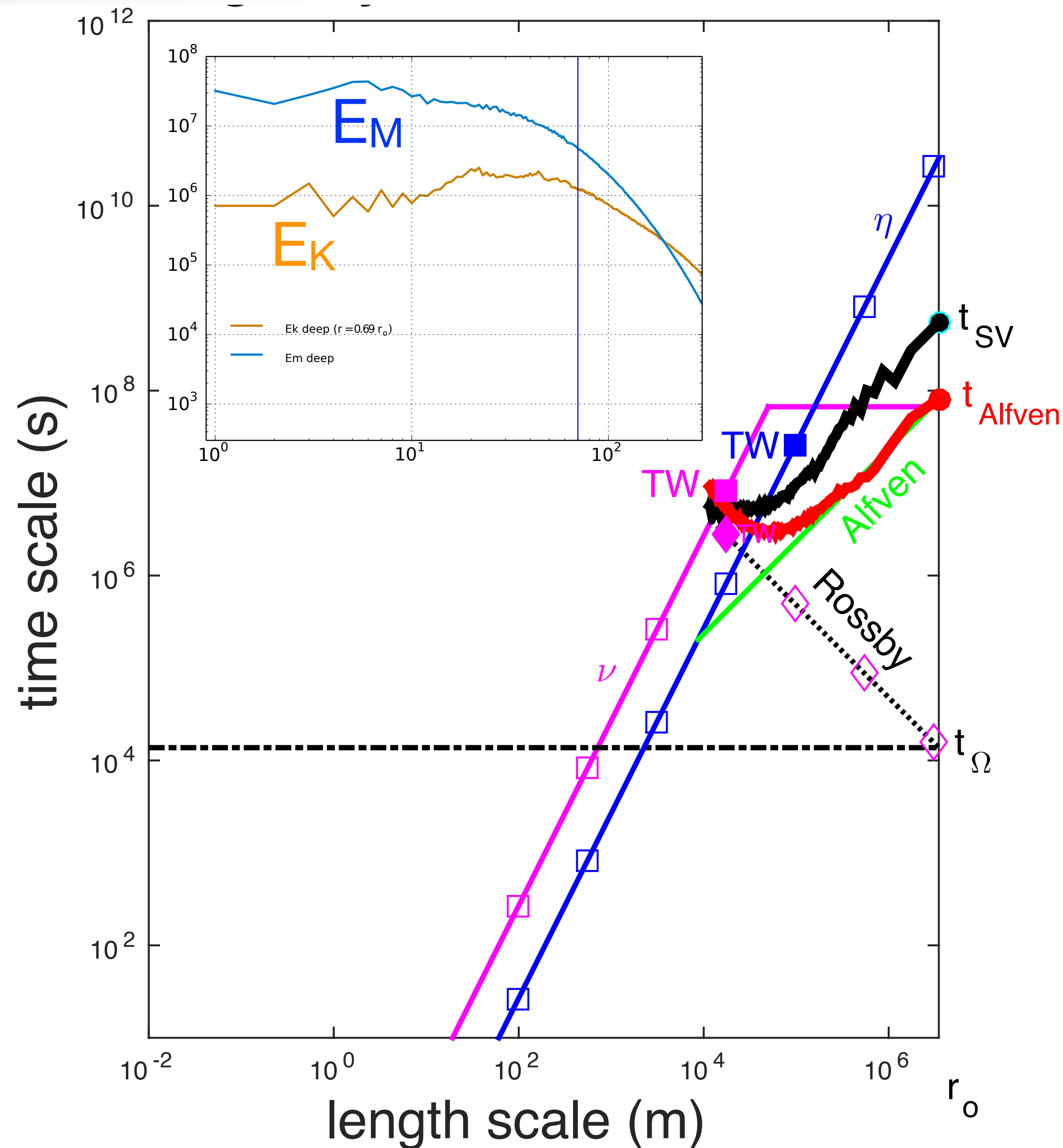
- In the Earth's core, **both rotation** and **magnetic field** play a leading role. We need to include both ingredients in our *tau-ell* regime diagrams.

The Earth's core tau-ell regime diagram



- Inertial wave times are shorter than Alfvén wave time down to a few hundred meters. Therefore, we expect mostly QG flow, especially in the dynamo region.
- Small-scale magnetic field generation halts below a scale of about 10km, yielding a **magnetic dissipation** of a few TW.
- The flow probably remains **QG** at all scales. Viscous dissipation is negligible.

Comparison with the tau-ell diagram of a numerical simulation



- Numerical simulations are not yet able to reach the extreme parameters relevant for the Earth core ($E \sim 10^{-15}$, $Pm \sim 10^{-6}$).
- Nathanaël Schaeffer built the ***tau-ell*** diagram of his most extreme S2 numerical simulation shown earlier today. The viscous and magnetic scales, energies, and dissipation are not as separated as in the Earth's core. Nevertheless, the simulation seems to reach a regime similar to the one we envision for the core.

A few concluding words

- Turbulence in planetary cores remains to be understood and described on firmer grounds. We are **lacking experimental and numerical illustrations** of how velocity and magnetic fields organize themselves under planetary core conditions.
- I hope that the *tau-ell* approach I have presented can help us and help you explore new tracks and understand better what's going on deep beneath our feet.